Supporting Information (SI)

Controllable Encapsulation of Silver Nanoparticles by Porous Pyridine-Based Covalent Organic Frameworks for Efficient CO_2 Conversion Using Propargylic Amines

*Yize Zhang,[a] Xingwang Lan,[*a,b] Fanyong Yan,[b] Xingyue He,[a] Juan Wang,[a] Luis Ricardez-Sandoval,[c] Ligong Chen,[d] Guoyi Bai[*a]*

[a]Key Laboratory of Chemical Biology of Hebei Province, College of Chemistry and Environmental Science, Hebei University, Baoding, Hebei, 071002, P.R. China.

[b]Tianjin Key Laboratory of Green Chemical Engineering Process Engineering，Tiangong University, Tianjin, 300387, PR China

[c]Department of Chemical Engineering, University of Waterloo, Waterloo, ON, N2L 3G1, Canada.

[d]School of Chemical Engineering and Technology, Tianjin University, Tianjin 300350, P. R. China.

Corresponding Authors

E-mail: hxlxw@sina.cn (X. Lan), baiguoyi@hotmail.com (G. Bai)

Table of Contents

1. Experimental section.....S1

1.1 Materials.....S1

1.2 Synthesis of 1,3,5-tris-(4-aminophenyl)triazine (TAPT).....S1

1.3 Synthesis of 4,4'-pyridine-2,6-diyldibenzaldehyde (2,6-FPP).....S1

1.4 Synthesis of 4,4'-pyridine-3,5-diyldibenzaldehyde (3,5-FPP).....S2

1.5 Synthesis of propargylic amines S3

1.6 Procedure for the cycling test.....S3

1.7 Characterization S3

2. Characterization data of substrates and products.....S4

3. Supplementary results and discussion S8

Figure S1. FT-IR spectra of (a) 2,6-FPP-TAPT and (b) 3,5-FPP-TAPT as well as their corresponding monomers.....S9

Figure S2. ^{13}C CP-MAS NMR spectra of 2,6-FPP-TAPT and 3,5-FPP-TAPT.....S9

Figure S3. Raman spectra of 2,6-FPP-TAPT and 3,5-FPP-TAPT as well as their corresponding monomers. S10

Figure S4. XPS spectra of 2,6-FPP-TAPT: (a) survey spectrum, (b) C 1s, (c) N 1s. S10

Figure S5. XPS spectra of 3,5-FPP-TAPT: (a) survey spectrum, (b) C 1s, (c) N 1s S11

Figure S6. TGA analysis of (a) 2,6-FPP-TAPT and (b) 3,5-FPP-TAPT. S11

Figure S7. SEM images of (a) 2,6-FPP-TAPT and (b) 3,5-FPP-TAPT.....S12

Figure S8. (a) N_2 adsorption-desorption isotherms for the 2,6-FPP-TAPT and 3,5-FPP-TAPT at 77 K; (b) their pore size distribution determined by the NLDFT method.....S12

Figure S9. PXRD patterns of 2,6-FPP-TAPT and 3,5-FPP-TAPT. S13

Figure S10. PXRD patterns of Ag@2,6-FPP-TAPT and Ag@3,5-FPP-TAPT.....S14

Figure S11. EDS image of Ag@2,6-FPP-TAPT.....S15

Figure S12. EDS image of Ag@3,5-FPP-TAPT.....S15

Figure S13. FT-IR spectra of fresh and used Ag@2,6-FPP-TAPT and Ag@3,5-FPP-TAPT.....S16

Figure S14. Hot filtration experiment using Ag@2,6-FPP-TAPT and Ag@3,5-FPP-TAPT under room temperature for 10 h. S16

Figure S15. TEM images and particle size distribution of used (a-c) Ag@2,6-FPP-TAPT and (d-f) Ag@3,5-FPP-TAPT.....S17

Figure S16. The GC-MS spectra of ^{13}C-labeled **2a** and unlabeled **2a** produced from the carboxylative cyclization of 1a using $^{13}CO_2$ as substrate. S18

Figure S17. ^{1}H NMR spectral changes on different systems in $CDCl_3$. S19

Figure S18. CO_2 sorption isotherms of 2,6-FPP-TAPT and Ag@2,6-FPP-TAPT at 298 K. S20

Figure S19. Continuous-flow setup (graphic and photographic representations) for the the carboxylative cyclization of *N*-benzylprop-2-yn-1-amine (**1a**) with CO_2. .....S20

Table S1. Comparison with previously reported catalytic systems.....S21

REFERENCES.....S22

Copies of NMR spectra.....S23

1. Experimental section

1.1 Materials

Trifluoroacetic acid (99%), 4-formylphenylboronic acid (99%), $Pd(PPh_3)_4$ (99%), 2,6-dibromopyridine (98%), and 3,5-dibromopyridine (98%) were purchased from Energy chemical Co., Ltd. Propargyl bromide (98%) and benzylamine derivatives (99%) were purchased from Shanghai Macklin Biochemical Co., Ltd. Mesitylene (98%) and 1,8-diazabicyclo[5.4.0]undec-7-ene (DBU) (98%) were purchased from *J&K* Scientific Co., Ltd. 4-Aminobenzonitrile (98%) was provided by Shanghai Aladdin Biochemical Co., Ltd. Other chemical reagents were purchased from local chemical suppliers. All chemical reagents were directly used without further purification.

1.2 Synthesis of 1,3,5-tris-(4-aminophenyl)triazine (TAPT)

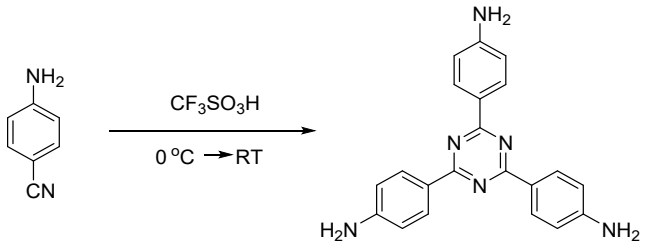

TAPT was synthesized according to previous report with minor modification.[1] Typically, trifluoromethanesulfonic acid (2 mL, 22.2 mmol) was dropwise added in a 50 mL reaction flask containing 4-aminobenzonitrile (772 mg, 6.53 mmol) at 0 °C. After the addition, the mixture was warmed to room temperature and stirred for a 24 h under Ar atmosphere. After completion, 20 mL H_2O was added to the mixture and then neutralized with 2M NaOH aqueous solution to form a precipitate. The collected yellow precipitate was filtered and washed with H_2O (2 × 50 mL), and then dried under vacuum at 60 °C. Finally, light yellow powder was obtained, affording to TAPT. ^{1}H-NMR (400 MHz, DMSO-d_6), δ_H (ppm): 8.36 (d, J=8.0, 6H), 6.7 (d, J=8.4, 6H), 5.9 (s, 6H). ^{13}C-NMR (100 MHz, DMSO-d_6), δ_C (ppm): 170.07, 153.49, 130.66, 123.42, 113.61.

1.3 Synthesis of 4,4'-pyridine-2,6-diyldibenzaldehyde (2,6-FPP)

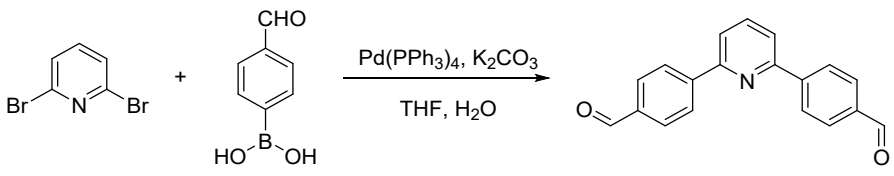

The 2,6-FPP was synthesized according to previous report with minor modification.[2] Typically, a 50 mL reaction flask was charged with 2,6-dibromopyridine (237 mg, 1.0 mmol), 4-formylphenylboronic acid (350 mg, 2.33 mmol), K_2CO_3 (1.0 g, 7.2 mmol), THF (10 mL) and H_2O (2.0 mL). The mixture was bubbled with nitrogen for 10 min, and $Pd(PPh_3)_4$ (100 mg, 0.086 mmol) was added in the mixture, which was then stirred for 36 h at 70 °C under Ar atmosphere. After completion, the reaction mixture was cooled to room temperature, and following that 20 mL H_2O was added to the mixture, which was then extracted with $CHCl_2$ (3×20 mL). The collected organic phase was dried with anhydrous Na_2SO_4 and concentrated to obtain the crude product. The crude product was further purified by column chromatography (PE/DCM = 2:1, then neat DCM) and finally obtain a white solid (215 mg, 75 %). ^{1}H-NMR (400 MHz, $CDCl_3$), δ_H (ppm): 10.11 (s, 2H), 8.33 (d, J = 8.4 Hz, 4H), 8.03 (d, J = 8.4 Hz, 4H), 7.95 (dd, J = 8.4 Hz, J = 6.8 Hz, 1H), 7.85 (d, J = 7.6 Hz, 2H). ^{13}C-NMR (100 MHz, $CDCl_3$), δ_C (ppm): 191.99, 155.68, 144.53, 138.08, 136.60, 130.19, 127.57, 120.37.

1.4 Synthesis of 4,4'-pyridine-3,5-diyldibenzaldehyde (3,5-FPP)

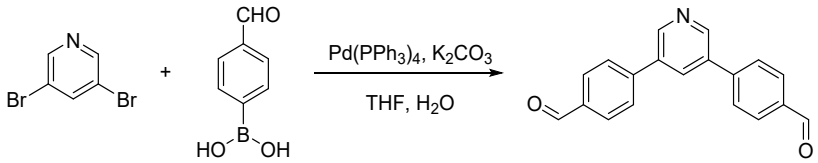

The 2,6-FPP was synthesized according to previous report with minor modification.[2] Typically, a 50 mL reaction flask was charged with 2,6-dibromopyridine (237 mg, 1.0 mmol), 4-formylphenylboronic acid (350 mg, 2.33 mmol), K_2CO_3 (1.0 g, 7.2 mmol), THF (10 mL) and H_2O (2.0 mL). The mixture was bubbled with nitrogen for 10 min, and $Pd(PPh_3)_4$ (100 mg, 0.086 mmol) was added in the mixture, which was then stirred for 36 h at 70 °C under Ar atmosphere. After completion, the reaction mixture was cooled to room temperature, and following that 20 mL H_2O was added to the mixture, which was then extracted with $CHCl_2$ (3 × 20 mL). The collected organic phase was dried with anhydrous Na_2SO_4 and concentrated to obtain the crude product. The crude product was further purified by column chromatography (neat DCM, then DCM/CH_3OH = 100/1) and finally obtain a white solid (207mg, 72 %). ^{1}H-NMR (400 MHz, $CDCl_3$), δ_H (ppm): 10.11 (s, 2H), 8.94 (d, J = 2.4 Hz, 2H), 8.15 (t, J = 2.4 Hz, 1H), 8.05 (d, J = 8.4 Hz, 4H), 7.84 (d, J = 8.4 Hz,

4H). ^{13}C-NMR (100 MHz, $CDCl_3$), δ_C (ppm): 191.65, 147.94, 136.06, 135.63, 133.33, 130.57, 127.93.

1.5 Synthesis of propargylic amines

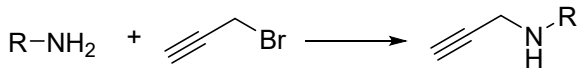

1a-1i

Propargylic amines 1a-1i were synthesized according to previous report with minor modification.[3] In a typical experiment, propargyl bromide (3 mL, 39.3 mmol) was added dropwise with 30 min to amines (0.162 mol) in a 50 mL round bottom flask at 0 ºC. Then after that, the mixture was stirred at room temperature for 12 h. After completion, the mixture was diluted with 40 mL ethyl ether, and then the organic phase was washed with $NaHSO_4$ saturated solution (3 × 40 mL). After collected organic phase dried with anhydrous Na_2SO_4, the organic phase was concentrated and further purified by column chromatography (PE/EA = 7/1, then PE/EA = 3/1), yellow oil was finally obtained.

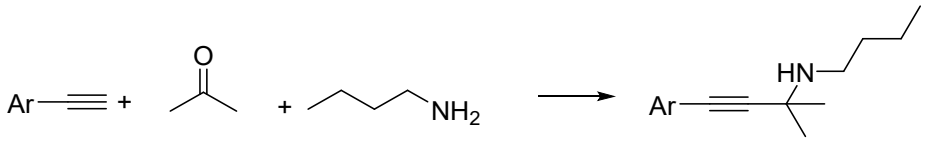

1j and 1k

Propargylic amines **1j** and **1k** were synthesized according to previous report with minor modification.[4] In a typical experiment, the reaction flask containing CuI (114 mg, 0.6 mmol) was charged with alkyne (2.0 mmol), acetone (116 mg, 2.0 mmol), and *n*-butylamine (146 mg, 2.0 mmol) under Ar atmosphere. The reaction mixture was stirred at 75 °C for 12 h. After the reaction was completed, the crude product was directedly purified by column chromatography (PE/EA = 20/1, then PE/EA = 3/1) and a yellow oil was finally obtained.

1.6 Procedure for the cycling test

After the reaction, the catalyst was collected by filtration and washed with CH_3OH (3 × 5 mL), and then dried under vacuum at 60 °C. And then the recovered catalyst was directly used as the recycled catalyst in next cycling test.

1.7 Characterization

The Fourier transformed infrared spectroscopy (FT-IR) was a Nicolet iS10 spectrometer. ^{13}C cross-polarization magic angle spinning (CP-MAS) spectra were recorded on a Bruker Avance III 400M NMR Spectrometer. Raman spectra were collected on the LabRAM HR Evolution with 633 nm laser. X-ray photoelectron spectroscopy (XPS) spectra were obtained in a Thermo ESCALAB 250 Xi spectrometer. Thermogravimetric analysis (TGA) was performed on STA449C/QMS403C/TENSOR27. The binding energies were referenced to the C 1s line at 284.8 eV from adventitious carbon. The powder X-ray diffraction (XRD) patterns of the samples were collected on a Bruker D8 Advance Powder X-ray diffractometer with Cu Kα radiation. The loading content of Ag species in the catalysts was determined by inductively coupled plasma-mass spectrometry (ICP-MS; Varian Vista MPX). The morphologies of the samples were investigated on a scanning electron microscopy (SEM, Hitachi SU8010) and a transmission electron microscopy (TEM, JEOL JEM-2100F). The CO_2 adsorption-desorption isotherms were measured at 298 K using an Autosorb-iQ-MP.

2. Characterization data of substrates and products

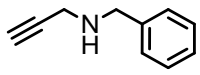

1a: pale yellow oil. ^1H-NMR (400 MHz, $CDCl_3$), δ_H (ppm): 7.36-7.25 (m, 5H), 3.88 (s, 2H), 3.43 (d, J = 2.8 Hz, 2H), 2.26 (t, J = 2.4 Hz, 1H), 1.73 (s, 1H). ^{13}C-NMR (100 MHz, $CDCl_3$), δ_C (ppm): 139.36, 128.44, 128.41, 127.16, 82.05, 71.57, 52.25, 37.31.

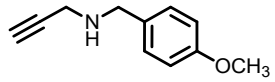

1b: pale yellow oil. ^1H-NMR (400 MHz, $CDCl_3$), δ_H (ppm): 7.26 (d, J = 8.4 Hz, 2H), 6.86 (d, J = 8.4 Hz, 2H), 3.82 (s, 2H), 3.80 (s, 3H), 3.41 (d, J = 2.4 Hz, 2H), 2.26 (t, J = 2.4 Hz, 1H) , 1.63 (s, 1H). ^{13}C-NMR (100 MHz, $CDCl_3$), δ_C (ppm): 158.82, 131.38, 129.72, 129.67, 113.81, 113.81, 82.10, 71.64, 55.32, 51.61, 37.14.

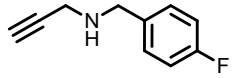

1c: pale yellow oil. ^1H-NMR (400 MHz, $CDCl_3$), δ_H (ppm): 7.29-7.33 (m, 2H), 7.01 (t, J = 8.8 Hz, 2H), 3.84 (s, 2H), 3.40 (d, J = 2.4Hz, 2H), 2.27 (t, J = 2.8 Hz, 1H), 1.49 (s, 1H). ^{13}C-NMR (100 MHz, $CDCl_3$), δ_C (ppm): 160.81, 135.09, 130.02, 129.94, 115.32, 115.11, 81.93, 71.68, 51.40, 37.18.

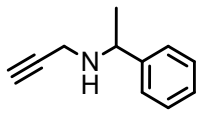

1d: pale yellow oil. ^{1}H-NMR (400 MHz, $CDCl_3$), δ_H (ppm): 7.39-7.24 (m, 5H), 4.02(q, J = 6.4 Hz, 1H), 3.35 (d, J = 2.4 Hz, 1H), 3.16 (d, J = 2.4 Hz, 1H), 2.22 (t, J = 2.4 Hz, 1H), 1.76 (s, 1H), 1.37(d, J = 6.8 Hz, 3H). ^{13}C-NMR (400 MHz, $CDCl_3$), δ_C (ppm): 144.24, 128.51, 127.23, 126.88, 82.11, 71.33, 56.31, 35.85, 23.87.

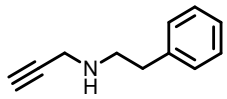

1e: pale yellow oil. ^{1}H-NMR (400 MHz, $CDCl_3$), δ_H (ppm): 7.32-7.219 (m, 5H), 3.43 (q, J = 6.4 Hz, 2H), 2.29 (d, J = 2.4 Hz, 2H), 2.82 (d, J = 2.4 Hz, 2H), 2.2 (t, J = 2.4 Hz, 2H), 1.36 (s, 1H). ^{13}C-NMR (100 MHz, $CDCl_3$), δ_C (ppm): 139.69, 128.70, 128.49, 126.23, 81.95, 71.41, 49.73, 38.09, 36.10.

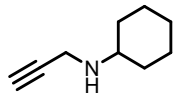

1f: pale yellow oil. ^{1}H-NMR (400 MHz, $CDCl_3$), δ_H (ppm): 3.46 (d, J = 2.4 Hz, 2H), 2.65 (tt, J = 10.4 Hz, 1H), 2.20 (t, J = 2.4 Hz, 1H), 1.87-1.84 (m, 2H), 1.75-1.72 (m, 2H), 1.64-1.61 (m, 2H), 1.35-1.02 (m, 6H). ^{13}C-NMR (100 MHz, $CDCl_3$), δ_C (ppm): 82.52, 70.99, 54.93, 35.09, 33.01, 26.08, 24.81.

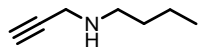

1g: pale yellow oil. ^{1}H-NMR (400 MHz, $CDCl_3$), δ_H (ppm): 3.45 (d, J = 2.4 Hz, 2H), 2.72 (t, J = 6.8 Hz, 2H), 2.24 (t, J = 2.4 Hz, 1H), 1.54-1.48 (m, 2H), 1.48-1.34 (m, 2H), 0.95 (t, J = 3.2 Hz, 3H). ^{13}C-NMR (100 MHz, $CDCl_3$), δ_C (ppm): 82.27, 71.20, 48.37, 38.17, 31.91, 20.42, 13.99.

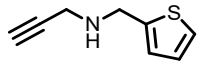

1h: pale yellow oil. ^{1}H-NMR (400 MHz, $CDCl_3$), δ_H (ppm): 7.26 (dd, J = 1.6 Hz, J = 4.8 Hz, 1H), 7.00-6.97 (m, 2H), 4.125 (s, 2H), 3.49 (d, J = 2.4 Hz, 2H), 2.29 (t, J = 2.4 Hz, 1H), 1.74 (s, 1H). ^{13}C-NMR (100 MHz, $CDCl_3$), δ_C (ppm): 142.95, 126.71, 125.54, 124.85, 81.77, 71.87, 46.75, 37.08.

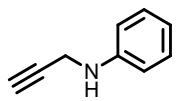

1i: pale yellow oil. ^{1}H-NMR (400 MHz, $CDCl_3$), δ_H (ppm): 7.22 (dd, J = 7.2 Hz, J = 8.4 Hz, 2H), 6.79 (t, J = 7.2 Hz, 1H), 6.69 (d, J = 8.0 Hz, 2H), 3.93 (d, J= 2.4 Hz, 2H), 2.21 (t, J= 2.4 Hz, 1H). ^{13}C-NMR (100 MHz, $CDCl_3$), δ_C (ppm): 146.71, 129.24, 118.74, 113.61, 80.92, 71.35, 33.70.

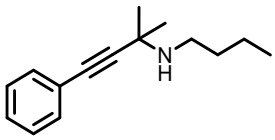

1j: black oil. ^{1}H-NMR (400 MHz, $CDCl_3$), δ_H (ppm): 7.40 (dd, J = 4.4 Hz, J = 7.6 Hz, 2H), 7.28 (dd, J = 2.0 Hz, J = 5.2 Hz, 3H), 2.78 (t, J = 3.2 Hz, 2H), 1.53-1.49 (m, 2H), 1.45 (s, 6H), 1.40-1.37 (m, 2H), 0.94 (t, J = 7.6 Hz, 3H). ^{13}C-NMR (100 MHz, $CDCl_3$), δ_C (ppm): 131.58, 128.20, 127.74, 123.48, 94.68, 81.90, 50.26, 44.08, 32.66, 29.63, 20.60, 14.04.

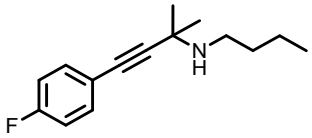

1k: black oil. ^{1}H-NMR (400 MHz, $CDCl_3$), δ_H (ppm): 7.39-7.35 (m, 2H), 7.00-6.96 (m, 2H), 2.77 (t, J = 7.2 Hz, 2H), 1.53-1.49 (m, 2H), 1.41 (s, 6H), 1.39-1.37 (m, 2H), 0.94 (t, J = 7.6 Hz, 3H). ^{13}C-NMR (100 MHz, $CDCl_3$), δ_C (ppm): 163.42, 160.95, 133.44, 133.36, 119.56, 119.52, 115.53, 115.31, 94.25, 80.91, 50.31, 44.07, 32.62, 29.61, 20.60, 14.02.

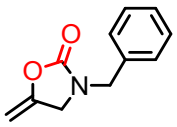

2a: pale yellow oil. ^{1}H-NMR (400 MHz, $CDCl_3$), δ_H (ppm): 7.37-7.26 (m, 5H), 4.74 (dd, J = 2.8 Hz, J = 5.6 Hz, 1H), 4.47 (s, 2H), 4.24 (dd, J = 2.4 Hz, J = 4.8 Hz, 1H), 4.02 (t, J = 2.4 Hz, 2H). ^{13}C-NMR (100 MHz, $CDCl_3$), δ_C (ppm): 155.65, 148.92, 134.95, 128.98, 128.26, 128.18, 86.80, 47.85, 47.22.

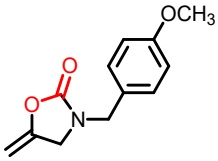

2b: pale yellow oil. ^{1}H-NMR (400 MHz, $CDCl_3$), δ_H (ppm): 7.20 (d, J = 8.4 Hz, 2H), 6.89 (d, J = 8.8 Hz, 2H), 4.72 (dd, J = 2.8 Hz, J = 5.6 Hz, 1H), 4.40 (s, 2H), 4.23 (dd, J = 2.4 Hz, J = 4.4 Hz, 1H), 4.00 (t, J = 2.4 Hz, 2H), 3.80 (s, 3H). ^{13}C-NMR (100 MHz, $CDCl_3$), δ_C (ppm): 159.52, 155.55, 149.02, 129.59, 126.95, 114.27, 86.66, 77.42, 77.10, 76.78, 55.31, 47.21, 47.06.

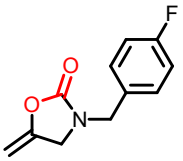

2c: pale yellow oil. ^{1}H-NMR (400 MHz, $CDCl_3$), δ_H (ppm): 7.29-7.25 (m, 2H), 7.05 (t, J = 8.8 Hz, 2H), 4.74 (dd, J = 2.8 Hz, J = 5.6 Hz, 1H), 4.44 (s, 2H), 4.27 (dd, J = 2.0 Hz, J = 4.8 Hz, 1H), 4.04 (t, J = 2.4 Hz, 2H). ^{13}C-NMR (100 MHz, $CDCl_3$), δ_C (ppm): 163.80, 161.34, 155.60, 148.83, 130.90, 130.87, 130.01, 129.93, 116.00, 115.79, 86.93, 47.16.

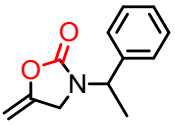

2d: pale yellow oil. ^{1}H-NMR (400 MHz, $CDCl_3$), δ_H (ppm): 7.40-7.30 (m, 5H), 5.26 (q, J = 7.2 Hz, 1H), 4.70 (dd, J = 2.8 Hz, J = 5.2 Hz, 1H), 4.22 (dd, J = 2.8 Hz, J = 5.2 Hz, 1H), 4.10 (m, 1H), 3.76 (m, 1H), 1.60 (d, J = 7.2 Hz, 3H). ^{13}C-NMR (100 MHz, $CDCl_3$), δ_C (ppm): 155.09, 149.21, 138.78, 128.84, 128.15, 126.97, 86.58, 51.30, 43.63, 16.39.

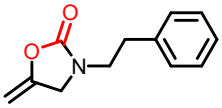

2e: pale yellow oil. ^{1}H-NMR (400 MHz, $CDCl_3$), δ_H (ppm): 7.22-7.20 (m, 5H), 4.69 (d, J = 2.8 Hz, 1H), 4.21 (d, J = 2.8 Hz, 1H), 3.99 (s, 2H), 3.55 (t, J = 7.2 Hz, 2H), 2.88 (t, J = 7.2 Hz, 2H). ^{13}C-NMR (100 MHz, $CDCl_3$), δ_C (ppm): 155.44, 149.00, 137.92, 128.75, 128.58, 126.78, 86.45, 48.34, 45.10, 33.87.

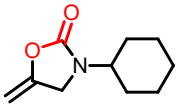

2f: pale yellow oil. ^{1}H-NMR (400 MHz, $CDCl_3$), δ_H (ppm): 4.72 (dd, J = 2.8 Hz, J = 5.6 Hz, 1H), 4.28 (dd, J = 2.4 Hz, J = 5.2 Hz, 1H), 4.14 (t, J = 2.4 Hz, 2H), 3.76-3.70 (m, 1H), 1.83-1.81 (m, 4H), 1.68 (d, J = 12.4 Hz, 1H), 1.38-1.29 (m, 4H), 1.14-1.01 (m, 1H). ^{13}C-NMR (100 MHz, $CDCl_3$), δ_C (ppm): 154.88, 149.62, 86.21, 52.31, 44.07, 30.23, 25.24, 25.19.

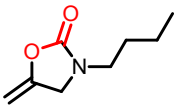

2g: pale yellow oil. ^{1}H-NMR (400 MHz, $CDCl_3$), δ_H (ppm): 4.72 (d, J = 2.8 Hz, 1H), 4.29 (d, J = 2.8 Hz, 1H), 4.17 (t, J = 2.8 Hz, 2H), 3.01 (t, J = 7.2 Hz, 2H), 1.58-1.51 (m, 2H), 1.40-1.31 (m, 2H),

0.95 (t, J = 7.2 Hz, 3H), 1.38-1.29 (m, 4H), 1.14-1.01 (m, 1H). ^{13}C-NMR (100 MHz, $CDCl_3$), δ_C (ppm): 155.59, 149.20, 86.37, 47.78, 43.46, 29.28, 19.77, 13.64.

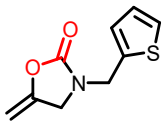

2h: pale yellow oil. ^{1}H-NMR (400 MHz, $CDCl_3$), δ_H (ppm): 7.30-7.27 (m, 1H), 7.02-6.98 (m, 2H), 4.74 (d, J = 2.8 Hz, 1H), 4.65 (s, 2H), 4.27 (d, J = 2.8 Hz, 1H), 4.11 (t, J = 2.4 Hz, 2H). ^{13}C-NMR (100 MHz, $CDCl_3$), δ_C (ppm): 155.17, 148.80, 137.05, 127.47, 127.17, 126.27, 86.96, 47.06, 42.20.

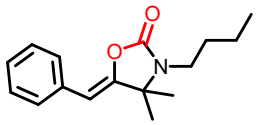

2j: yellow oil. ^{1}H-NMR (400 MHz, $CDCl_3$), δ_H (ppm): 7.58 (d, J = 7.2 Hz, 2H), 7.32 (t, J = 8.0 Hz, 2H), 7.20 (t, J = 7.6 Hz, 1H), 5.45 (s, 1H), 3.21 (t, J = 8.0 Hz, 2H), 1.70-1.64 (m, 2H), 1.49 (s, 6H), 1.41-1.35 (m, 2H), 0.96 (t, J = 7.2 Hz, 3H). ^{13}C-NMR (100 MHz, $CDCl_3$), δ_C (ppm): 154.19, 153.49, 133.66, 128.46, 128.27, 126.71, 100.38, 62.18, 40.41, 31.52, 27.62, 20.24, 13.76.

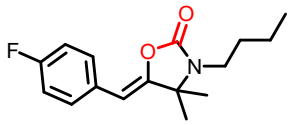

2k: yellow solid. ^{1}H-NMR (400 MHz, $CDCl_3$), δ_H (ppm): 7.56 (dd, J = 6.0 Hz, J = 8.8 Hz, 2H), 7.01 (t, J = 9.2 Hz, 2H), 5.42 (s, 1H), 3.20 (t, J = 8.0 Hz, 2H), 1.70-1.62 (m, 2H), 1.49 (s, 6H), 1.40-1.33 (m, 2H), 0.96 (t, J = 7.2 Hz, 3H). ^{13}C-NMR (100 MHz, $CDCl_3$), δ_C (ppm): 162.66, 160.21, 154.08, 153.12, 153.10, 129.92, 129.84, 115.45, 115.24, 99.31, 62.15, 40.42, 31.51, 27.60, 20.24, 13.75.

3. Supplementary results and discussion

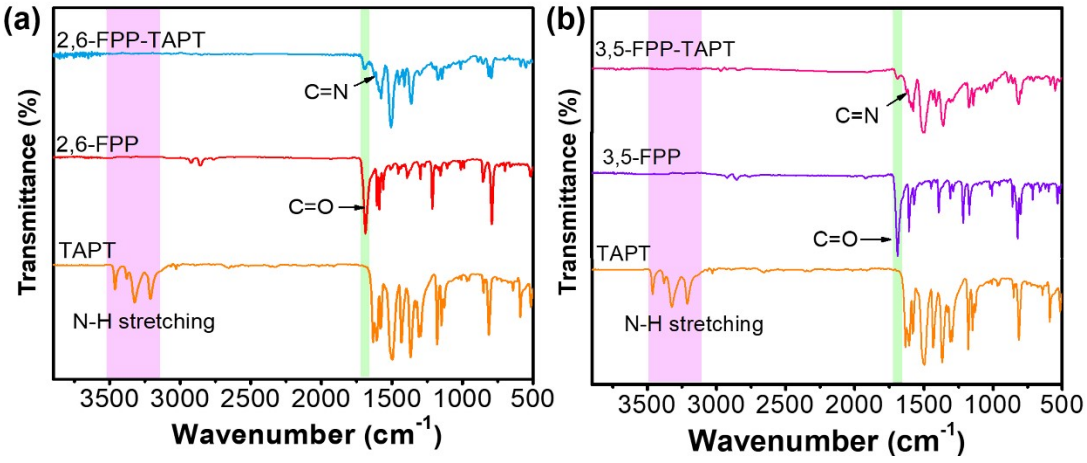

Figure S1. FT-IR spectra of (a) 2,6-FPP-TAPT and (b) 3,5-FPP-TAPT as well as their corresponding monomers.

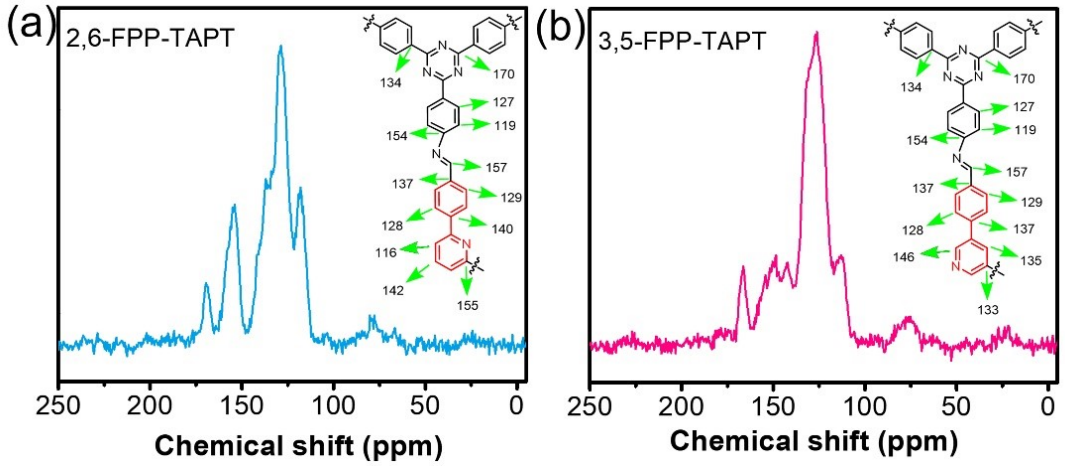

Figure S2. ^{13}C CP-MAS NMR spectra of 2,6-FPP-TAPT and 3,5-FPP-TAPT.

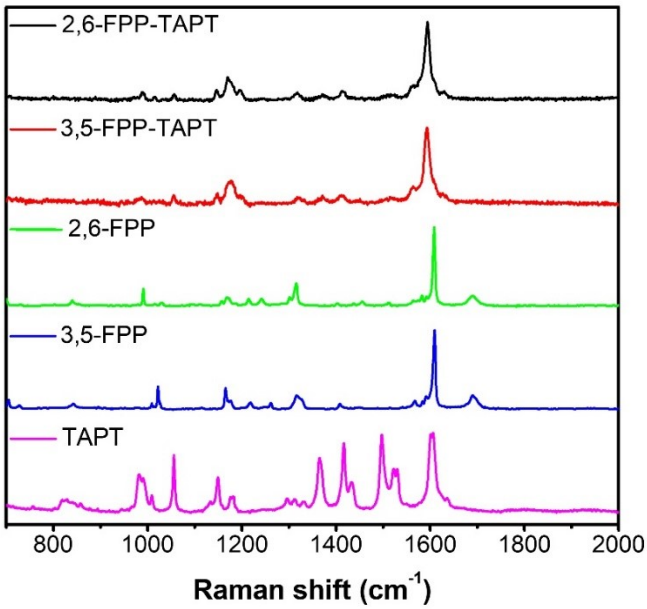

Figure S3. Raman spectra of 2,6-FPP-TAPT and 3,5-FPP-TAPT as well as their corresponding monomers.

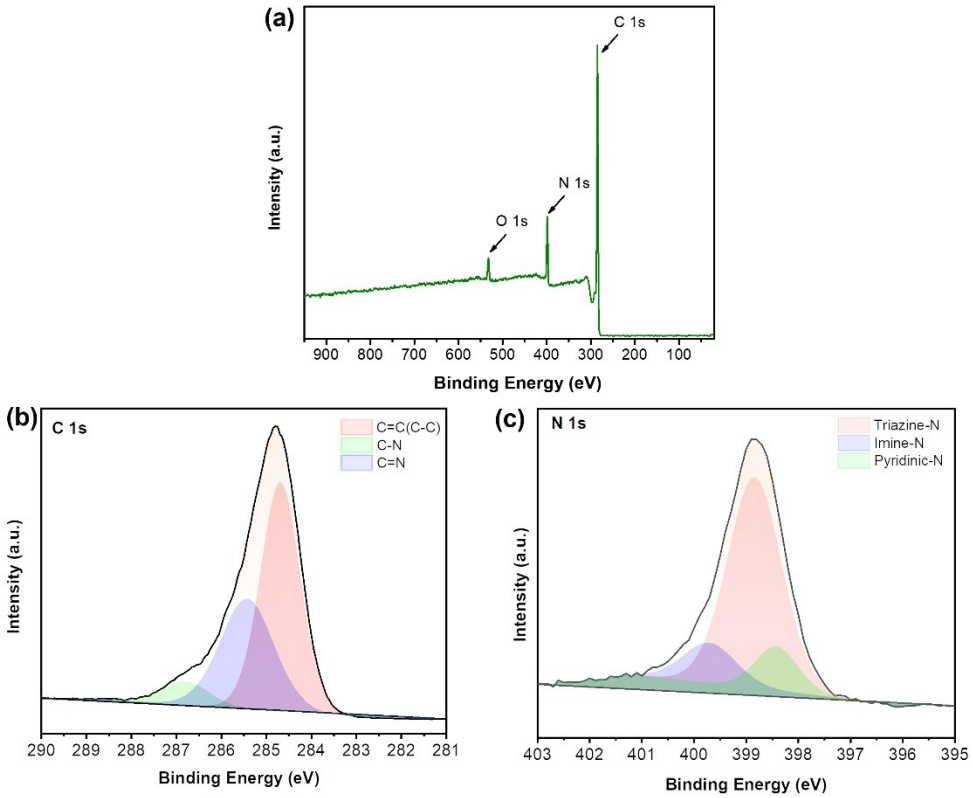

Figure S4. XPS spectra of 2,6-FPP-TAPT: (a) survey spectrum, (b) C 1s, (c) N 1s.

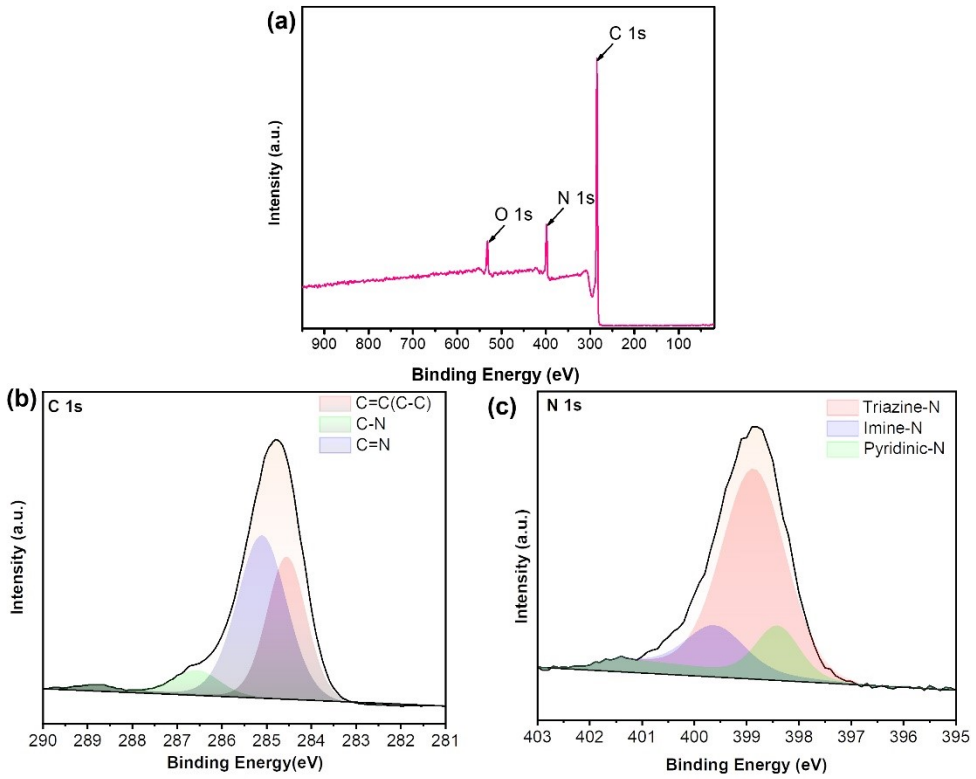

Figure S5. XPS spectra of 3,5-FPP-TAPT: (a) survey spectrum, (b) C 1s, (c) N 1s

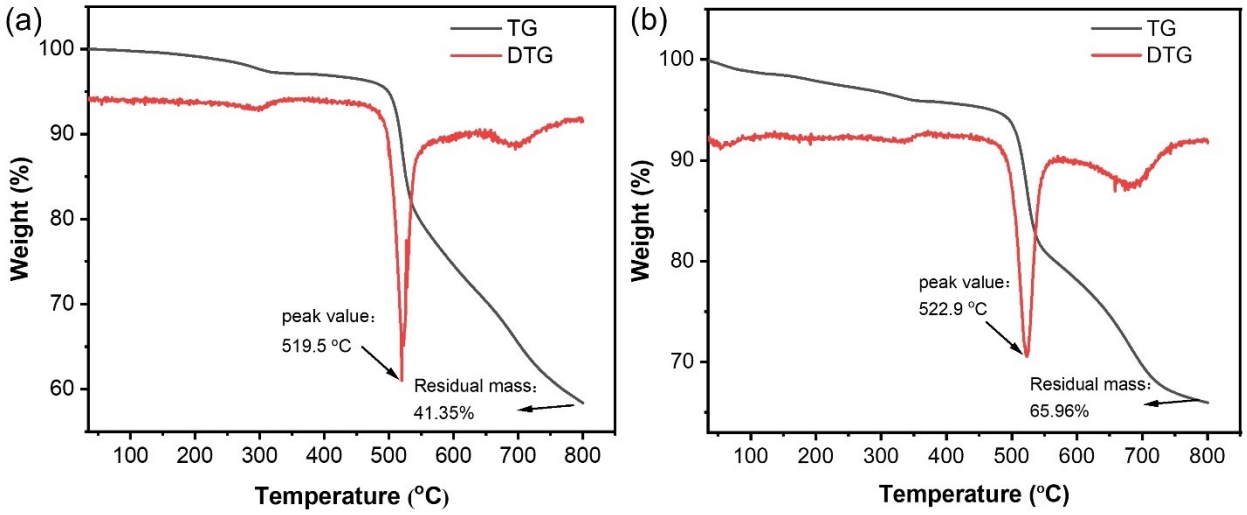

Figure S6. TGA analysis of (a) 2,6-FPP-TAPT and (b) 3,5-FPP-TAPT.

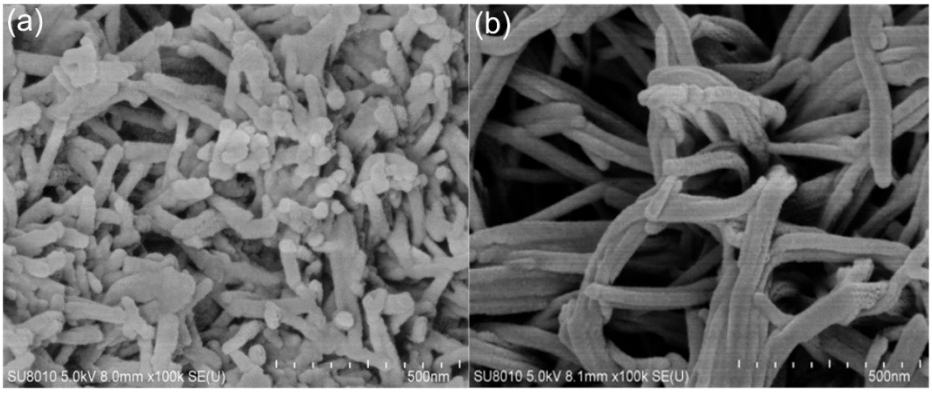

Figure S7. SEM images of (a) 2,6-FPP-TAPT and (b) 3,5-FPP-TAPT.

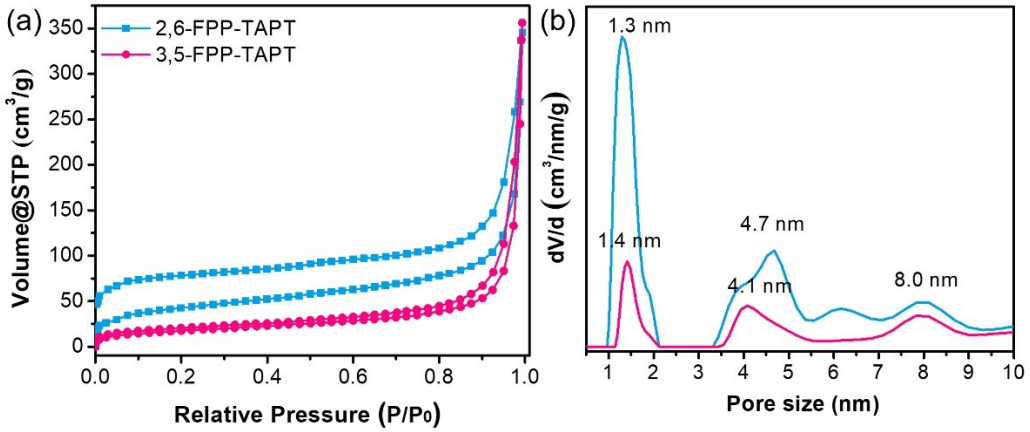

Figure S8. (a) N_2 adsorption-desorption isotherms for the 2,6-FPP-TAPT and 3,5-FPP-TAPT at 77 K; (b) their pore size distribution determined by the NLDFT method.

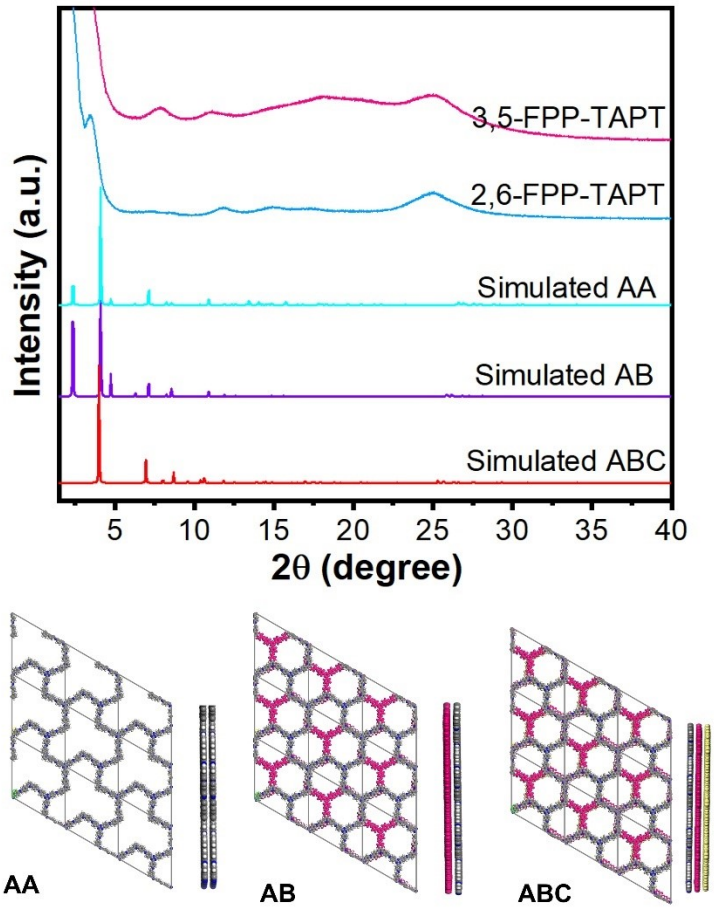

Figure S9. PXRD patterns of 2,6-FPP-TAPT and 3,5-FPP-TAPT. Comparison of the experimental PXRD of 2,6-FPP-TAPT profile and the stimulated stack profiles of AA, AB, and ABC modes. (e) Ideal unit cell representation and the supercell of 2,6-FPP-TAPT in the P1 space group by the universal force field.

PXRD pattern of 2,6-FPP-TAPT revealed only moderate crystallinity with reflections at 3.37°, 7.3°, 8.5°, 11.7°, and 14.8°. We chose the 2,6-FPP-TAPT to compare its experimental PXRD pattern with their simulated patterns based on the AA, AB, ABC stacking modes. The position and intensity of experimentally observed curve cannot match with the AA and AB- modes, thus excluding their existence. Impressively, the ABC mode was the better match with the experimental profile although some deviations were still observed.

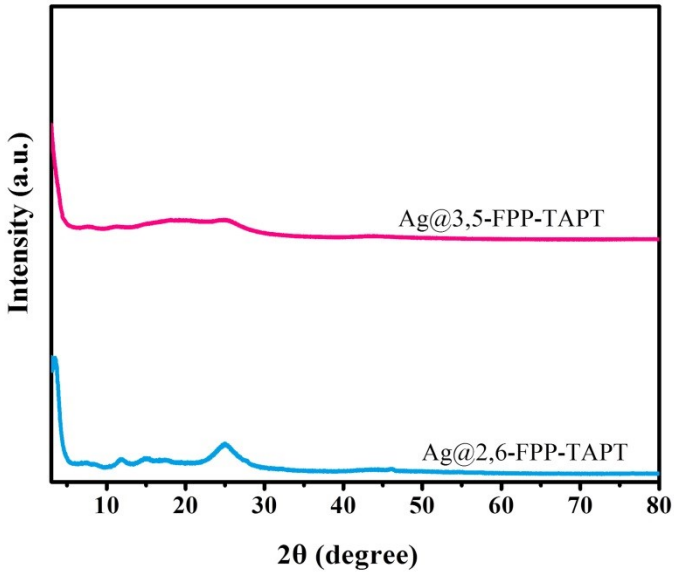

Figure S10. PXRD patterns of Ag@2,6-FPP-TAPT and Ag@3,5-FPP-TAPT.

The Ag@2,6-FPP-TAPT and Ag@3,5-FPP-TAPT were also tested by PXRD measurement. As shown in Figure S10, the PXRD patterns of Ag@2,6-FPP-TAPT and Ag@3,5-FPP-TAPT exhibit almost no change compared with the 2,6-FPP-TAPT and 3,5-FPP-TAPT. Also, no diffraction peaks corresponding to Ag NPs are observed, which can be possibly ascribed to too high dispersion or ultrasmall size of Ag NPs because of the confinement of 2,6-FPP-TAPT and 3,5-FPP-TAPT by the interaction between them. The PXRD results are consistent with TEM observations.

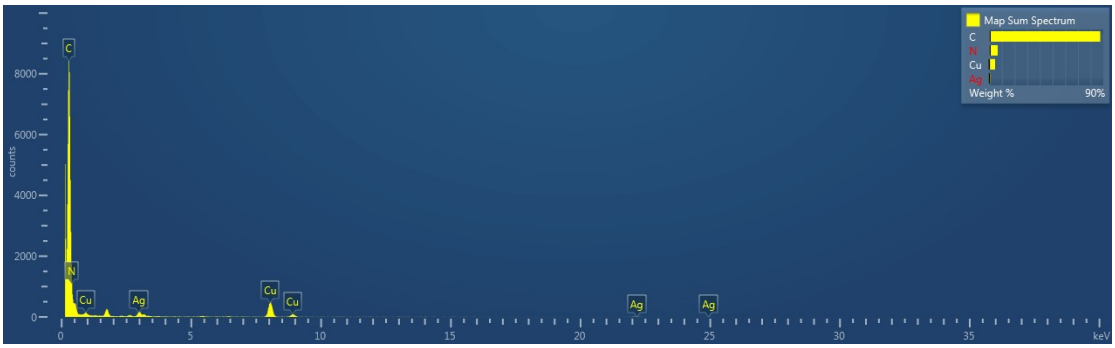

Element	Line Type	k Factor	Absorption Correction	Wt%	Wt% Sigma
C	K series	2.769	1.00	91.89	0.81
N	K series	3.515	1.00	7.02	0.77
Ag	K series	10.869	1.00	1.09	0.26

Figure S11. EDS image of Ag@2,6-FPP-TAPT

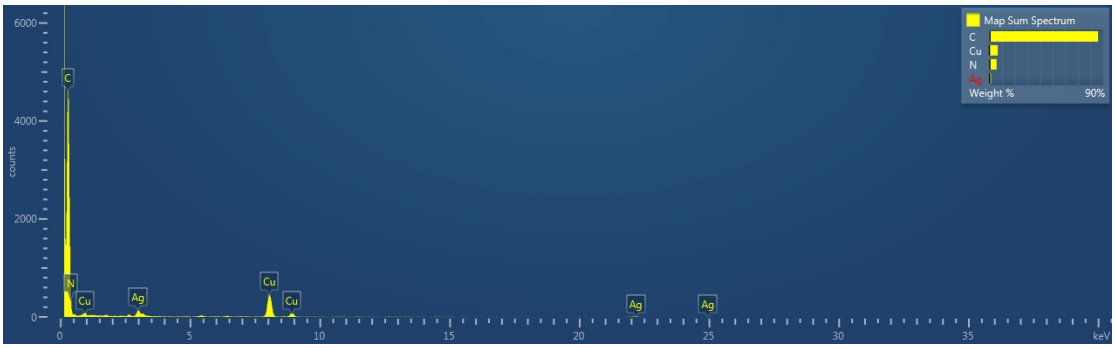

Element	Line Type	k Factor	Absorption Correction	Wt%	Wt% Sigma
C	K series	2.769	1.00	92.13	0.68
N	K series	3.515	1.00	6.30	0.59
Ag	K series	10.869	1.00	1.57	0.39

Figure S12. EDS image of Ag@3,5-FPP-TAPT.

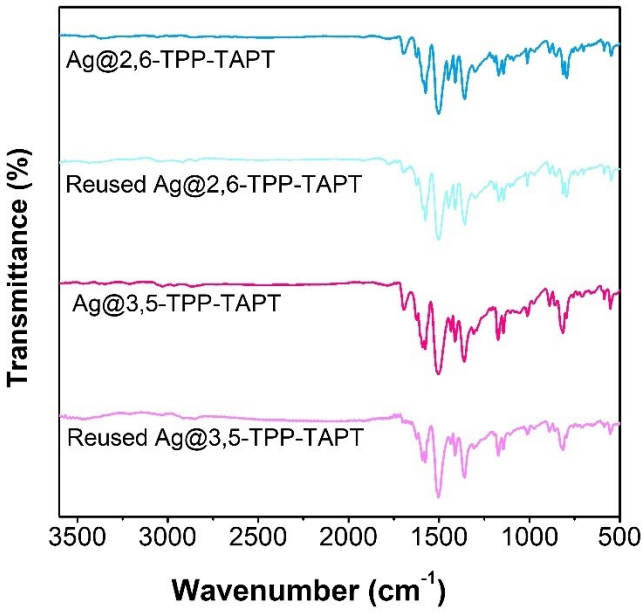

Figure S13. FT-IR spectra of fresh and used Ag@2,6-FPP-TAPT and Ag@3,5-FPP-TAPT.

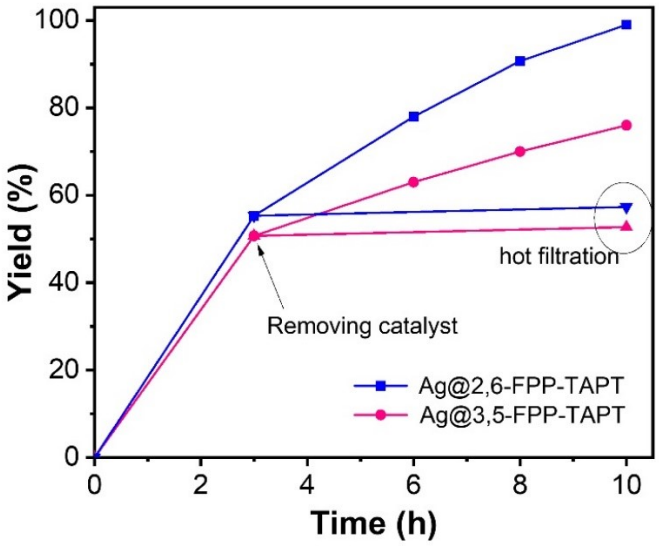

Figure S14. Hot filtration experiment using Ag@2,6-FPP-TAPT and Ag@3,5-FPP-TAPT under room temperature for 10 h.

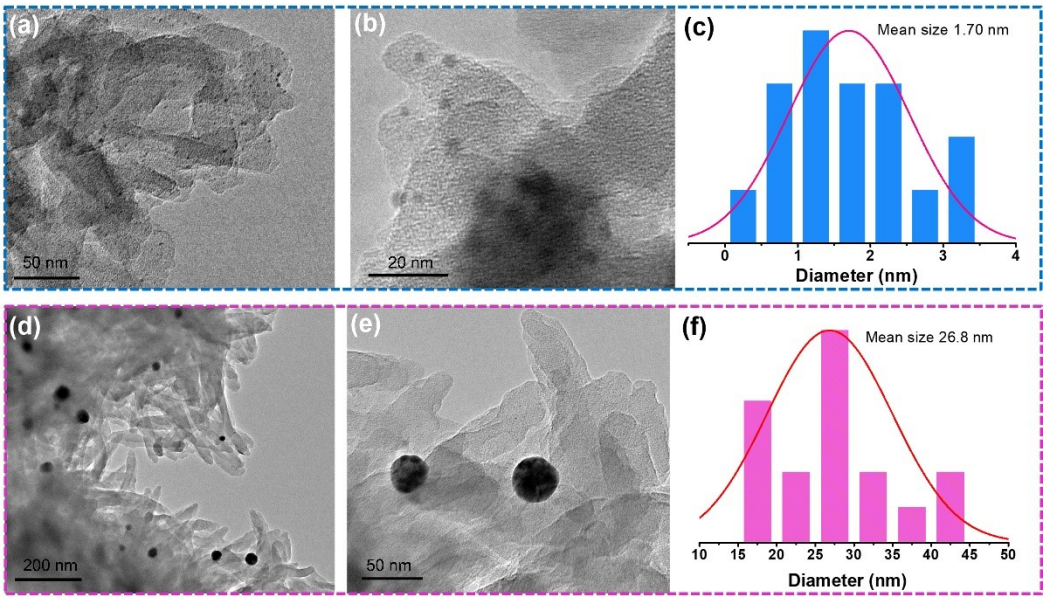

Figure S15. TEM images and particle size distribution of used (a-c) Ag@2,6-FPP-TAPT and (d-f) Ag@3,5-FPP-TAPT.

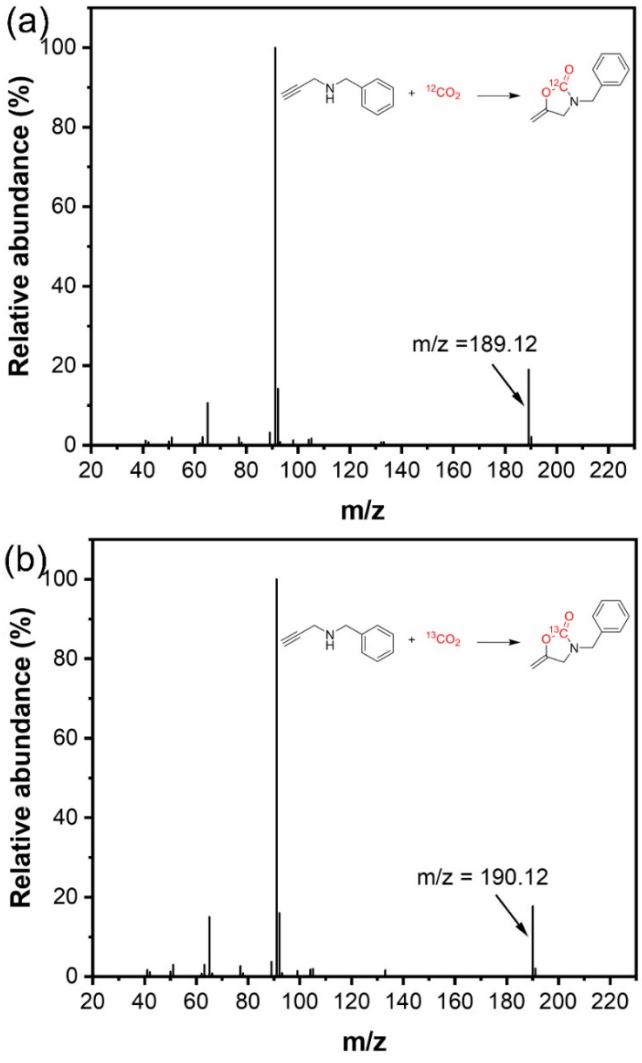

Figure S16. The GC-MS spectra of ^{13}C-labeled **2a** and unlabeled **2a** produced from the carboxylative cyclization of 1a using $^{13}CO_2$ as substrate.

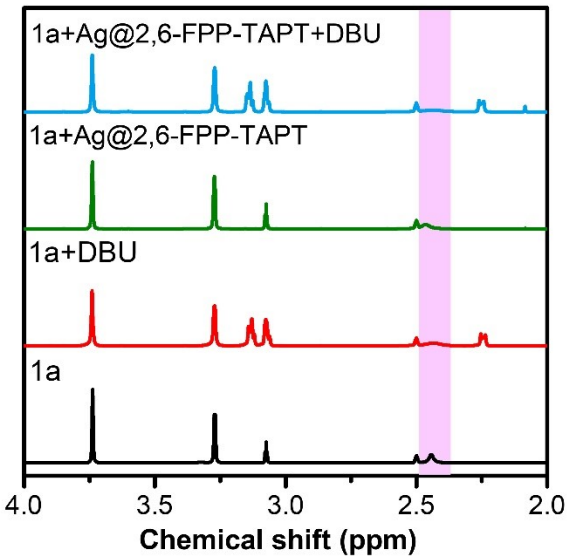

Figure S17. ^{1}H NMR spectral changes on different systems in d_6-DMSO.

As shown in Figure S17, in comparison to the ^{1}H NMR spectrum of the liquid **1a**, ^{1}H signal of the N-H group slightly shifted from δ 2.45 to 2.48 ppm after adding the Ag@2,6-FPP-TAPT; however, no significant change was observed in the characteristic signal shape, thus demonstrating that Ag@2,6-FPP-TAPT interacted with **1a** by Ag··NH hydrogen-bonding interaction[44] but without any activation. By contrast, the ^{1}H signal of the N-H group became dwarf even disappeared but no apparent shift was observed when adding DBU, indicating that the N-H group of **1a** was activated by DBU, which then reacted with CO_2 into the carbamate.

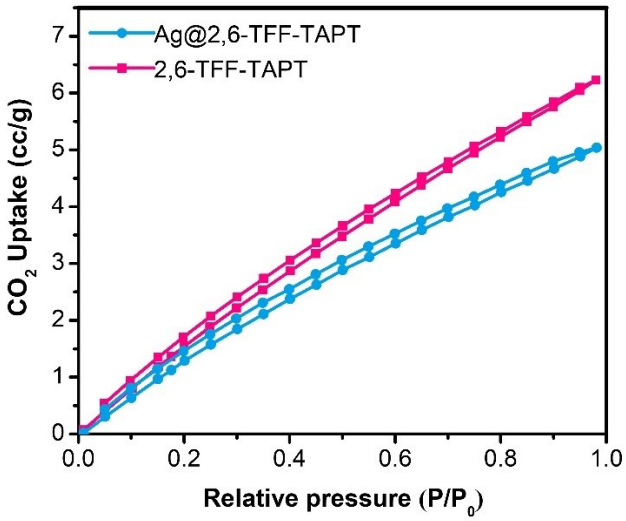

Figure S18. CO_2 sorption isotherms of 2,6-FPP-TAPT and Ag@2,6-FPP-TAPT at 298 K.

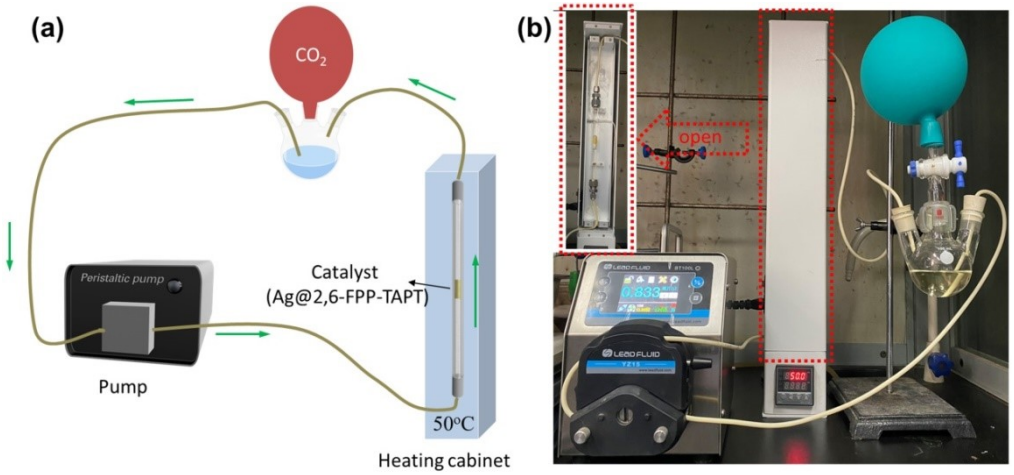

Figure S19. Continuous-flow setup (graphic and photographic representations) for the carboxylative cyclization of *N*-benzylprop-2-yn-1-amine (**1a**) with CO_2.

Table S1. Comparison with previously reported catalytic systems.

Entry	Cat. (mmol)	Substrate (mmol)	T (^oC)	Time (h)	Yield (%)	TON	TOF (h^{-1})	Ref.
1	CuI (0.1)	1	50	4	98	10	2	[5]
2	AgOAc(0.01)	0.5	25	7	95	48	7	[6]
3	$AgNO_3$(0.005)	1	60	2	94	188	94	[7]
4	$CoBr_2$(0.05)	0.5	80	9	99	10	1	[8]
5	$ZnCl_2(TBD)_2$ (0.05)	1	60	12	96	19	2	[9]
6	[DBUH][MIm] (1)	0.5	60	6	90	-	-	[10]
7	[Bmim][OAc] (0.25)	0.5	100	12	84	-	-	[11]
8	Ag_{27}-MOF (0.008)	0.8	25	6	97	97	16	[12]
9	TOS-Ag4 (0.008)	0.8	25	24	99	100	4	[13]
10	Zn_{116} (0.0027)	1	70	12	99	370	31	[3]
11	PdSCS (0.008)	0.8	80	16	99	100	6	[14]
12	Ag@TpPa-1 (0.008)	2.6	60	18	96	312	17	[15]
13	Ag@2,6-FPP-TAPT (0.00026)	0.5	50	2	>99	1928	964	**this work**

14	Ag@3,5-FPP-TAPT (0.00026)	0.5	50	2	91	1754	877	**this work**
15	Ag@2,6-FPP-TAPT (0.00026)	0.5	25	10	>99	1928	193	**this work**
16	Ag@3,5-FPP-TAPT (0.00026)	0.5	25	10	76	1465	147	**this work**

REFERENCES

[1] R. Gomes, P. Bhanja, A. Bhaumik, *Chem. Commun.* **2015**, 51, 10050-10053.

[2] M. Otte, M. Lutz, R. J. M. K. Gebbink, *Eur. J. Org. Chem.* **2017**, 2017, 1657-1661.

[3] C. S. Cao, S. M. Xia, Z. J. Song, H. Xu, Y. Shi, L. N. He, P. Cheng, B. Zhao, *Angew. Chem. Int. Ed.* **2020**, 132, 8664-8671.

[4] H. Wang, J. Ying, M. Lai, X. Qi, J.-B. Peng, X.-F. Wu, *Adv. Synth. Catal.* **2018**, 360, 1693-1703.

[5] Y. Zhao, J. Qiu, L. Tian, Z. Li, M. Fan, J. Wang, *ACS Sustain. Chem. Eng.* **2016**, 4, 5553-5560.

[6] S. Yoshida, K. Fukui, S. Kikuchi, T. Yamada, *Chem. Lett.* **2009**, 38, 786-787.

[7] M. Yoshida, T. Mizuguchi, K. Shishido, *Chem. Eur. J.* **2012**, 18, 15578-15581.

[8] Z.-H. Zhou, S.-M. Xia, S.-Y. Huang, Y.-Z. Huang, K.-H. Chen, L.-N. He, *J. CO_2 Util.* **2019**, 34, 404-410.

[9] X. Liu, M. Y. Wang, S. Y. Wang, Q. Wang, L. N. He, *ChemSusChem.* **2017**, 10, 1210-1216.

[10] J. Hu, J. Ma, Q. Zhu, Z. Zhang, C. Wu, B. Han, *Angew. Chem. Int. Ed.* **2015**, 54, 5399-403.

[10] J. Hu, J. Ma, Z. Zhang, Q. Zhu, H. Zhou, W. Lu, B. Han, *Green Chem.* **2015**, 17, 1219-1225.

[12] M. Zhao, S. Huang, Q. Fu, W. Li, R. Guo, Q. Yao, F. Wang, P. Cui, C. H. Tung, D. Sun, *Angew. Chem. Int. Ed.* **2020**, 59, 20031-20036.

[13] Z. Chang, X. Jing, C. He, X. Liu, C. Duan, *ACS Catal.* **2018**, 8, 1384-1391.

[14] P. Brunel, J. Monot, C. E. Kefalidis, L. Maron, B. Martin-Vaca, D. Bourissou, *ACS Catal.* **2017**, 7, 2652-2660.

[15] S. Ghosh, R. A. Molla, U. Kayal, A. Bhaumik, S. M. Islam, *Dalton Tran.* **2019**, 48, 4657-4666.

Copies of NMR spectra

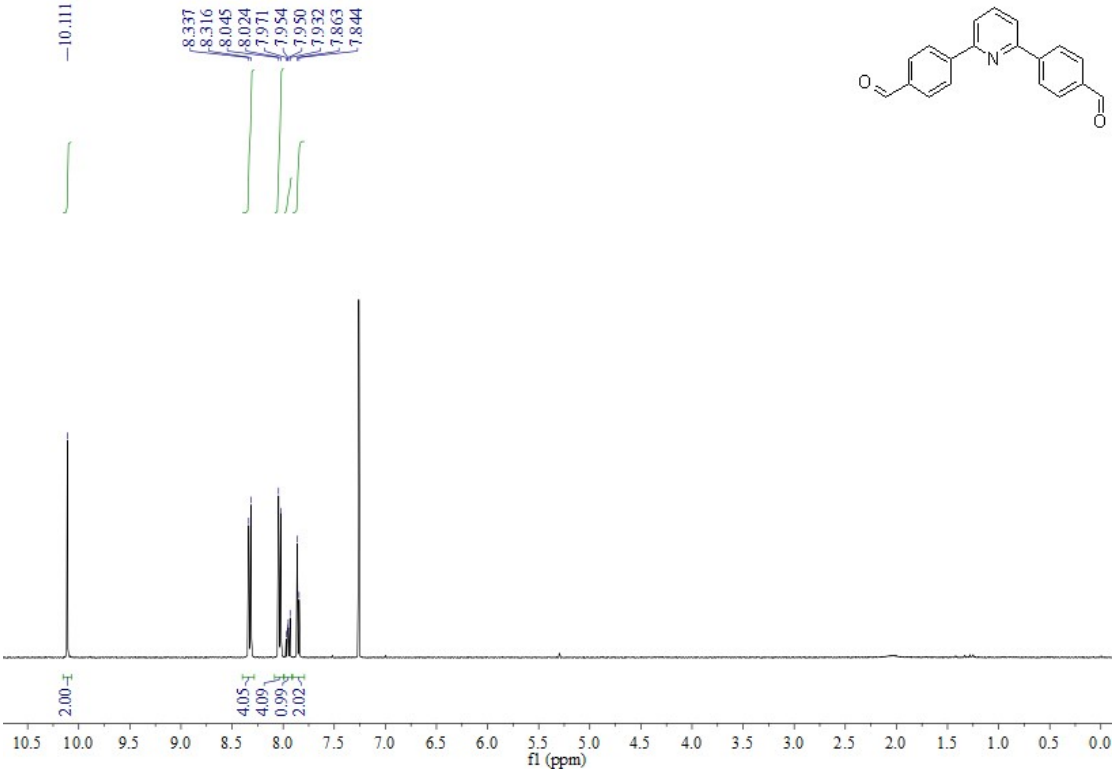

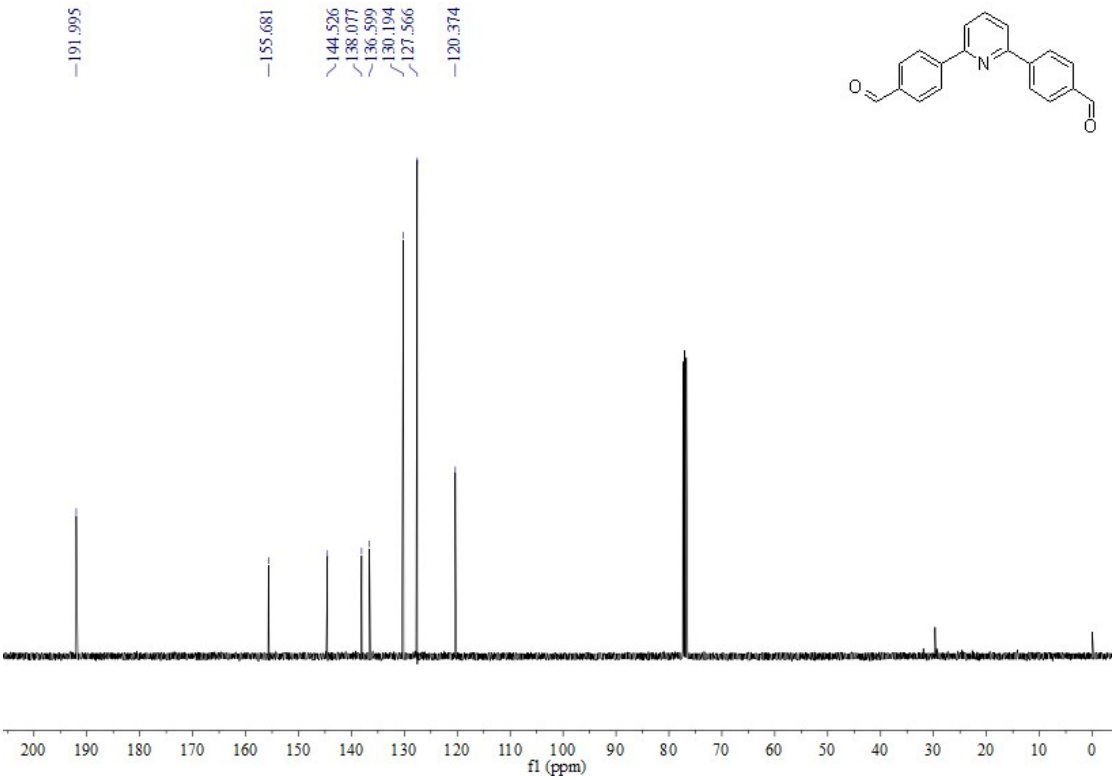

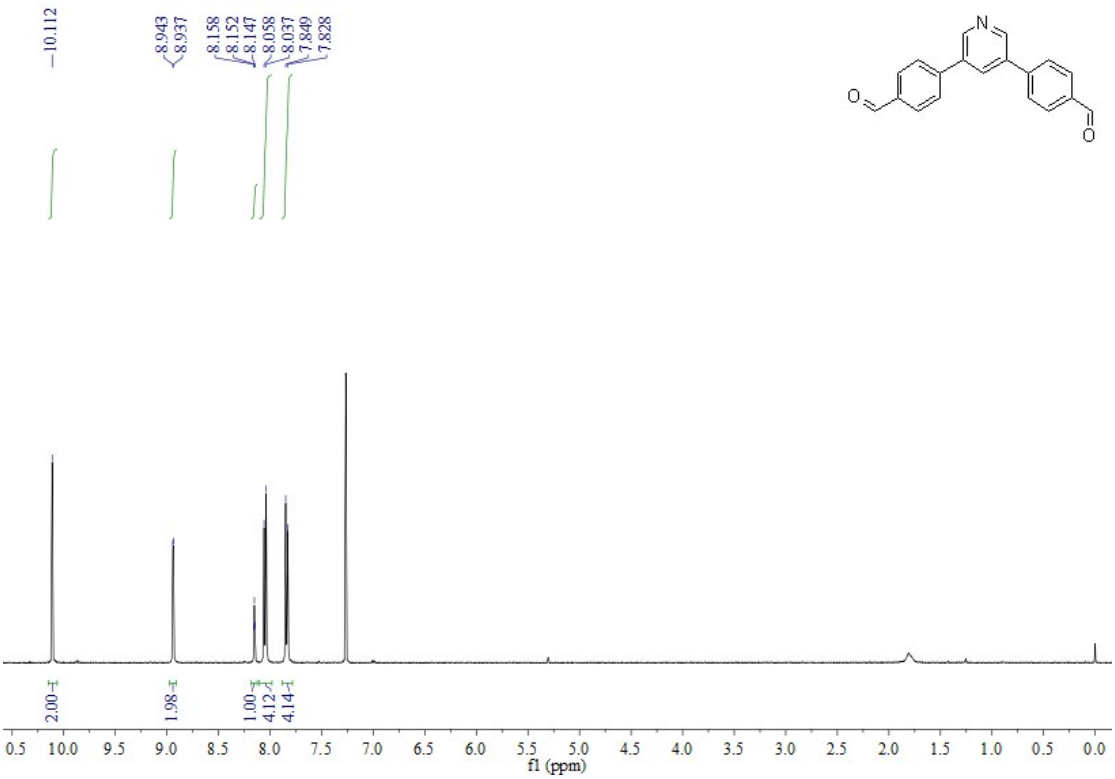
10.112
8.943
8.937
8.158
8.152
8.147
8.058
8.037
7.849
7.828
2.00
1.98
1.00
4.12
4.14
f1 (ppm)

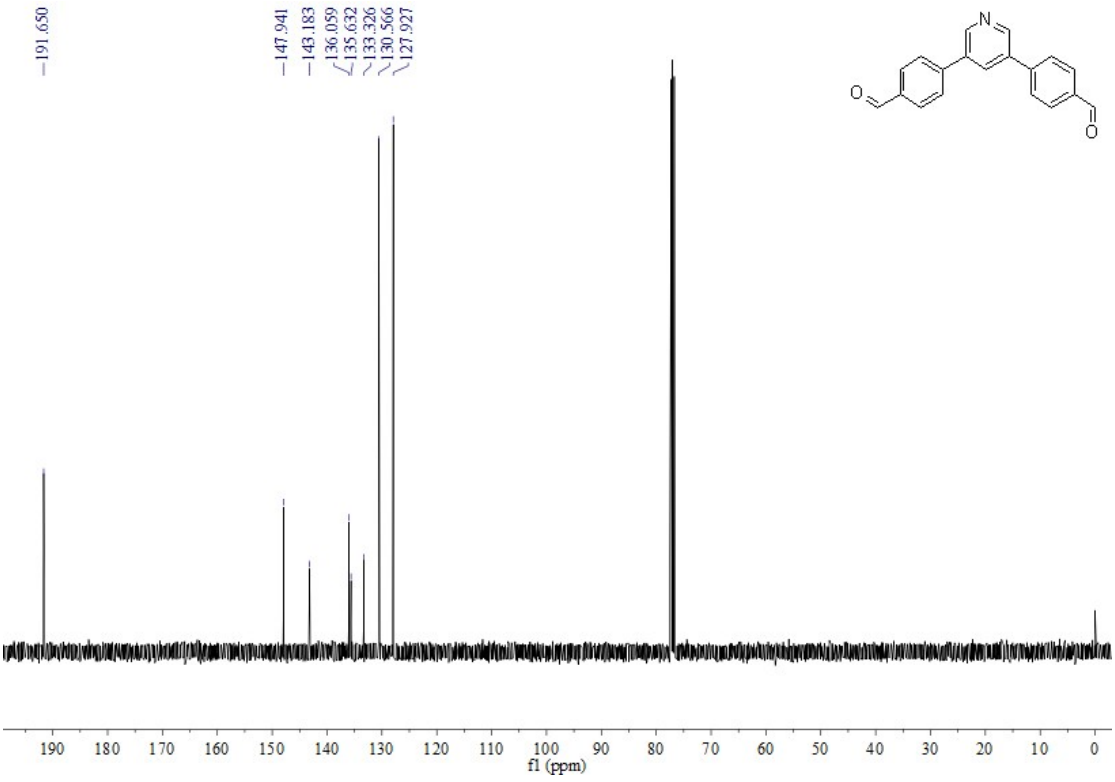
191.650
147.941
143.183
136.059
135.632
133.326
130.566
127.927
f1 (ppm)

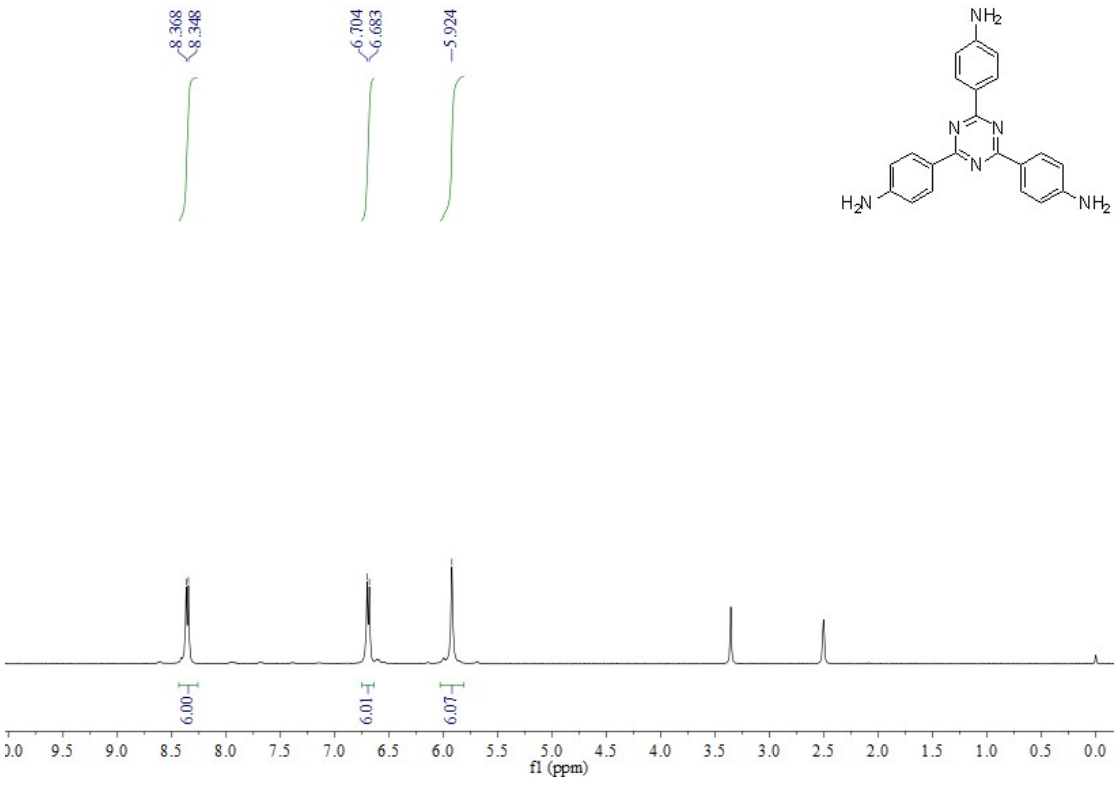
8.368
8.348
6.704
6.683
5.924
NH2
N
N
N
H2N
NH2
6.00
6.01
6.07
f1 (ppm)

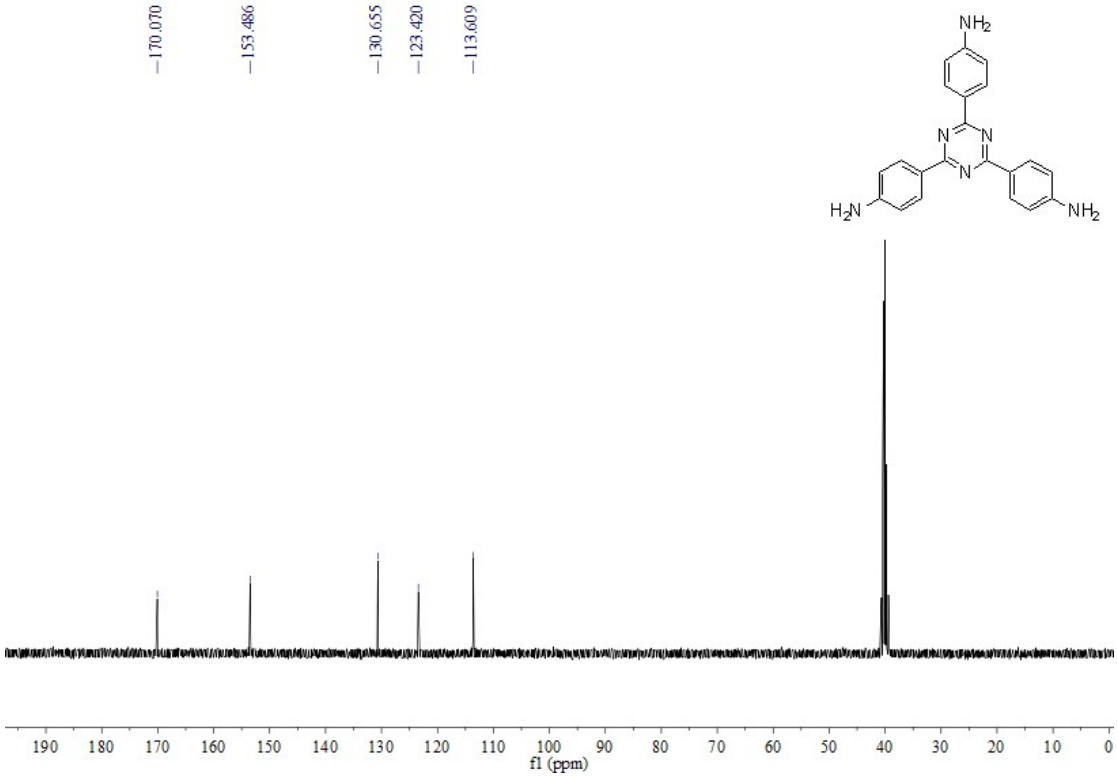
170.070
153.486
130.655
123.420
113.609
NH2
N
N
N
H2N
NH2
f1 (ppm)

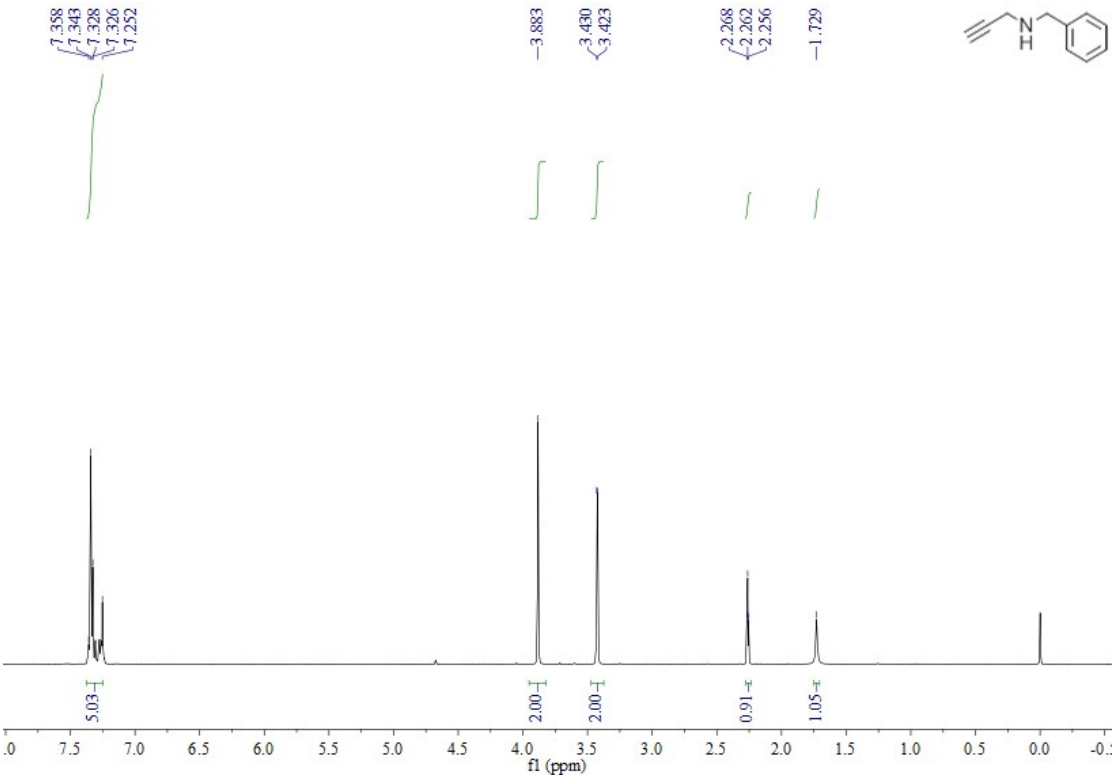
7.358
7.343
7.328
7.326
7.252
3.883
3.430
3.423
2.268
2.262
2.256
1.729
5.03
2.00
2.00
0.91
1.05
f1 (ppm)

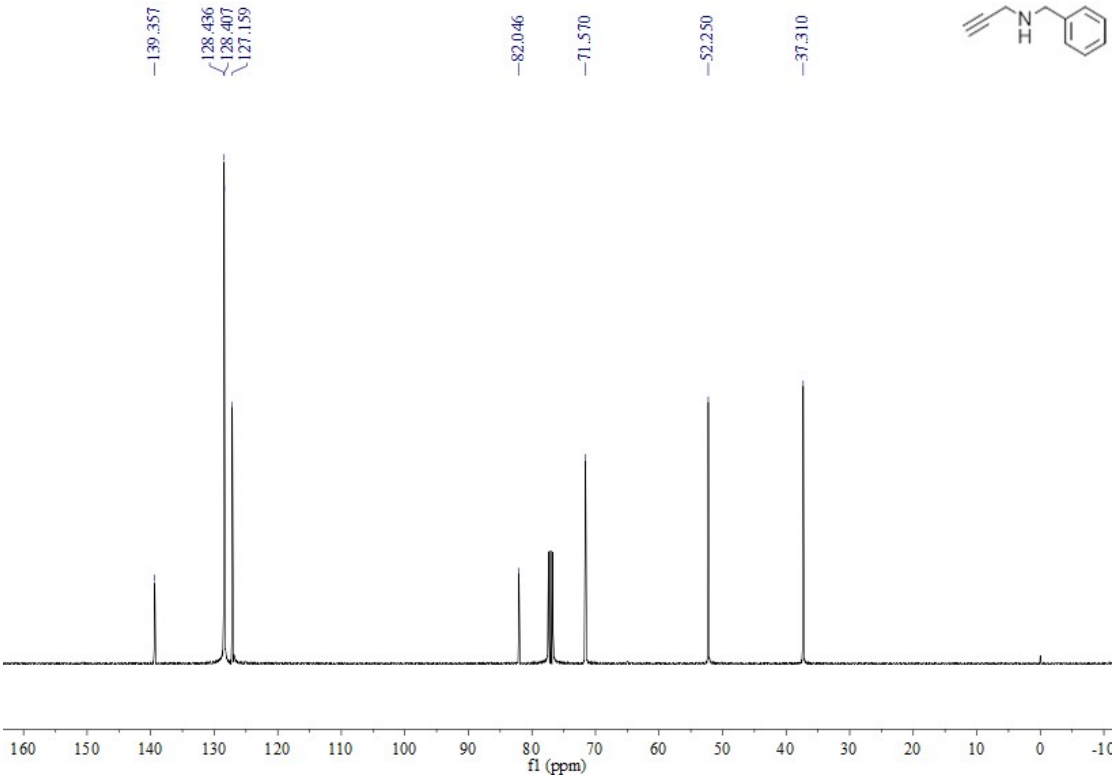
139.357
128.436
128.407
127.159
82.046
71.570
52.250
37.310
f1 (ppm)

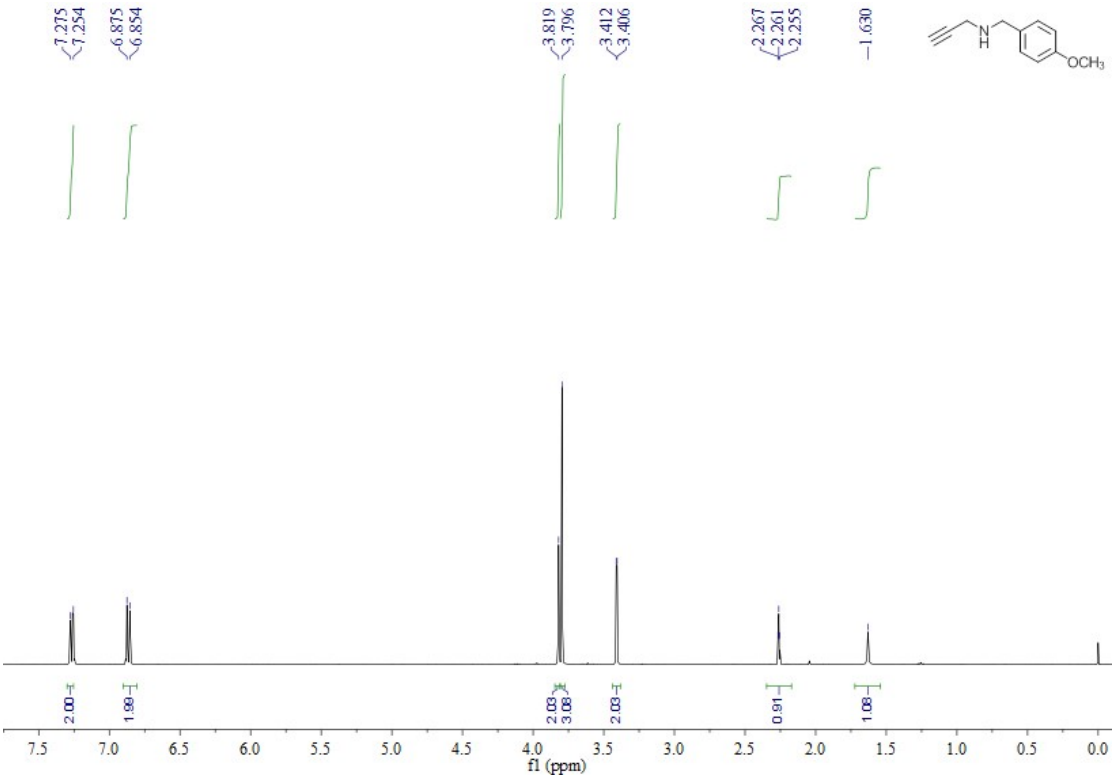
7.275
7.254
6.875
6.854
3.819
3.796
3.412
3.406
2.267
2.261
2.255
1.630
OCH3
2.00
1.99
2.03
3.08
2.03
0.91
1.08
f1 (ppm)

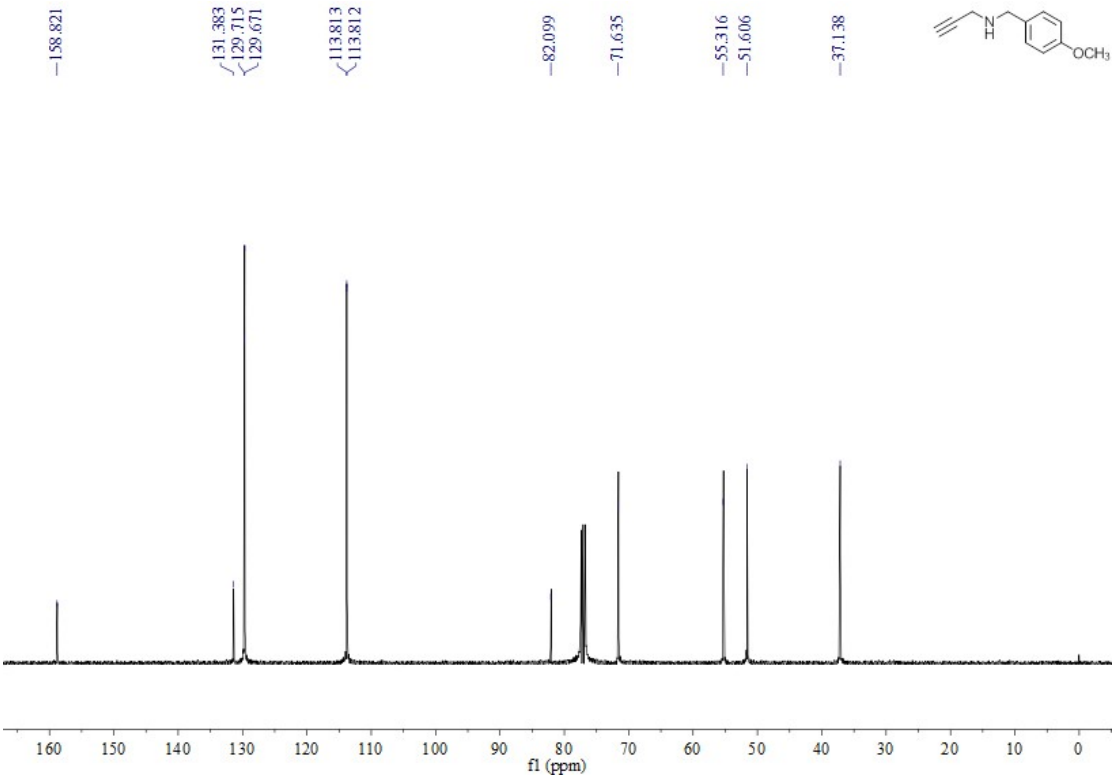
158.821
131.383
129.715
129.671
113.813
113.812
82.099
71.635
55.316
51.606
37.138
OCH3
f1 (ppm)

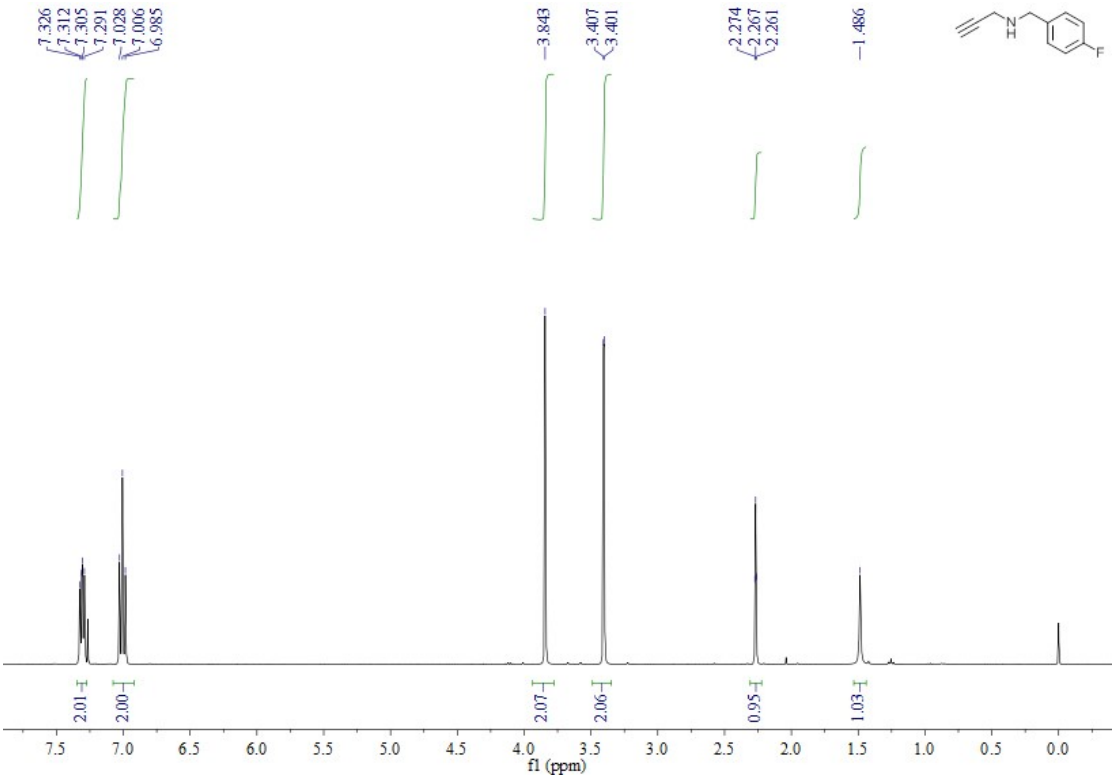
7.326
7.312
7.305
7.291
7.028
7.006
6.985
3.843
3.407
3.401
2.274
2.267
2.261
1.486
2.01
2.00
2.07
2.06
0.95
1.03
f1 (ppm)

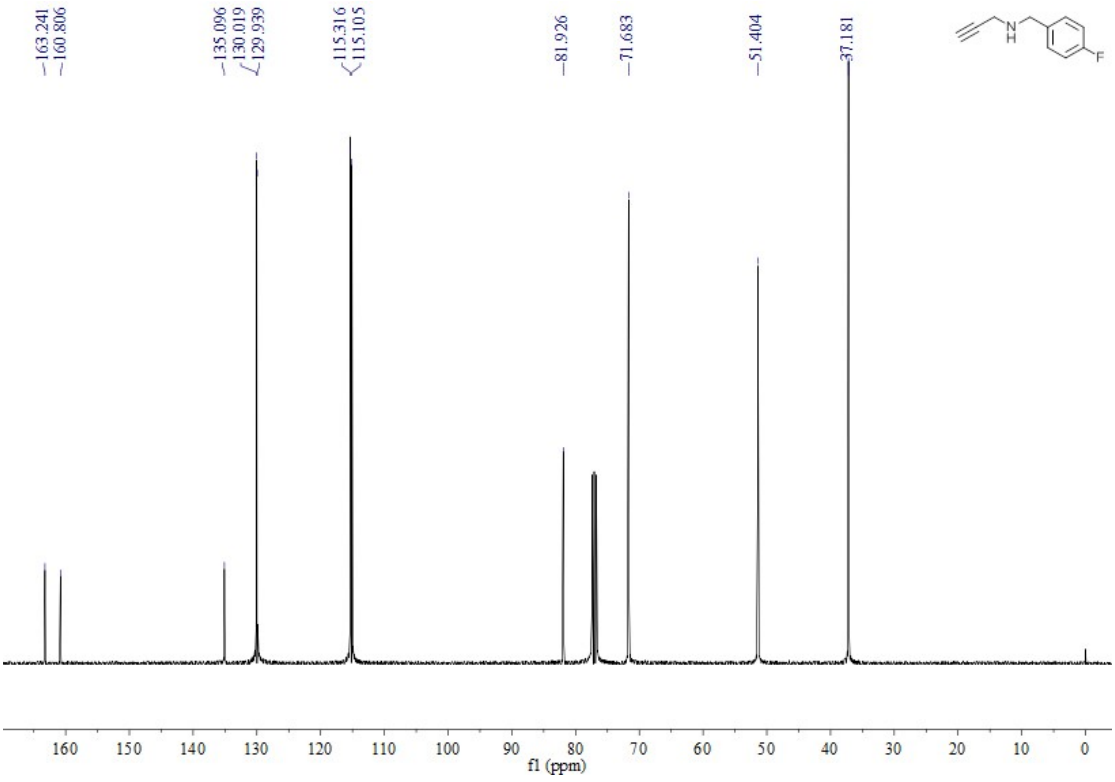
163.241
160.806
135.096
130.019
129.939
115.316
115.105
81.926
71.683
51.404
37.181
f1 (ppm)

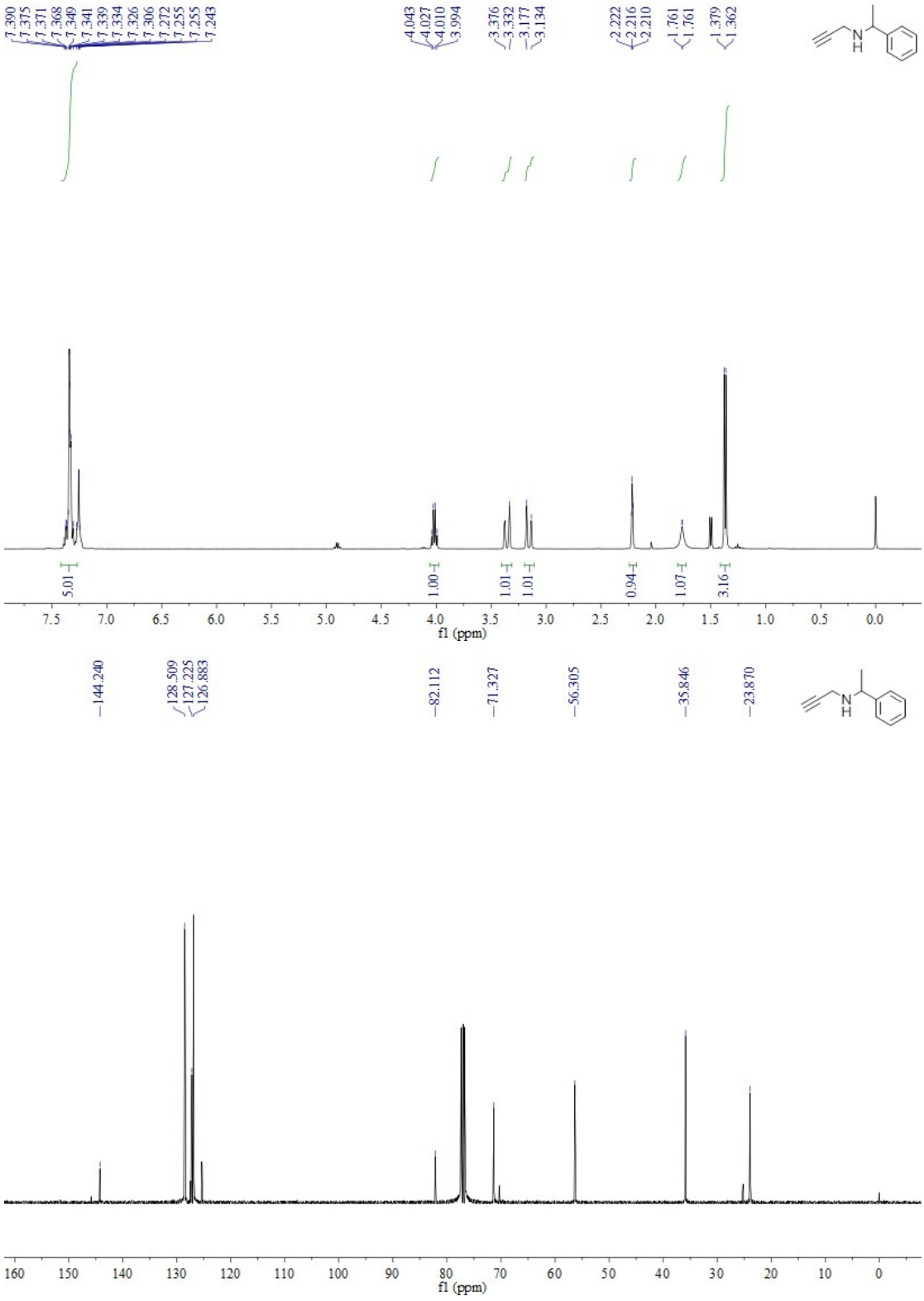
7.390
7.375
7.371
7.368
7.349
7.341
7.339
7.334
7.326
7.306
7.272
7.255
7.255
7.243
4.043
4.027
4.010
3.994
3.376
3.332
3.177
3.134
2.222
2.216
2.210
1.761
1.761
1.379
1.362
5.01
1.00
1.01
1.01
0.94
1.07
3.16
f1 (ppm)
144.240
128.509
127.225
126.883
82.112
71.327
56.305
35.846
23.870
f1 (ppm)

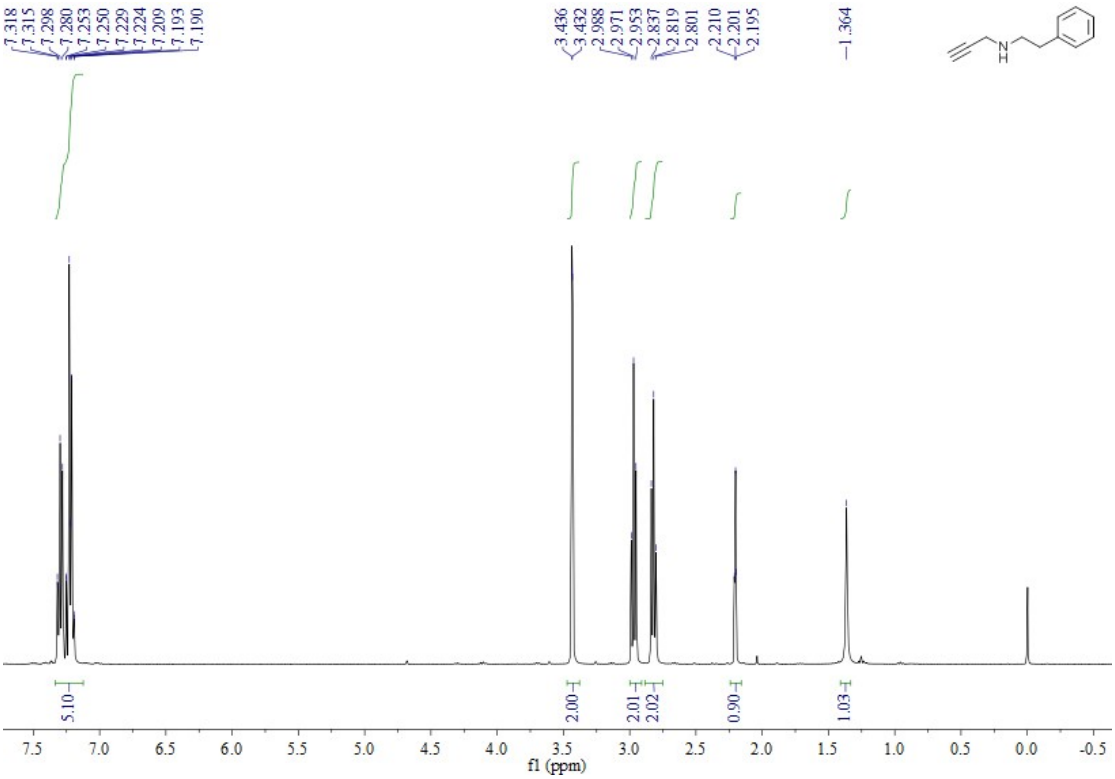
7.318
7.315
7.298
7.280
7.253
7.250
7.229
7.224
7.209
7.193
7.190
3.436
3.432
2.988
2.971
2.953
2.837
2.819
2.801
2.210
2.201
2.195
1.364
5.10
2.00
2.01
2.02
0.90
1.03
f1 (ppm)

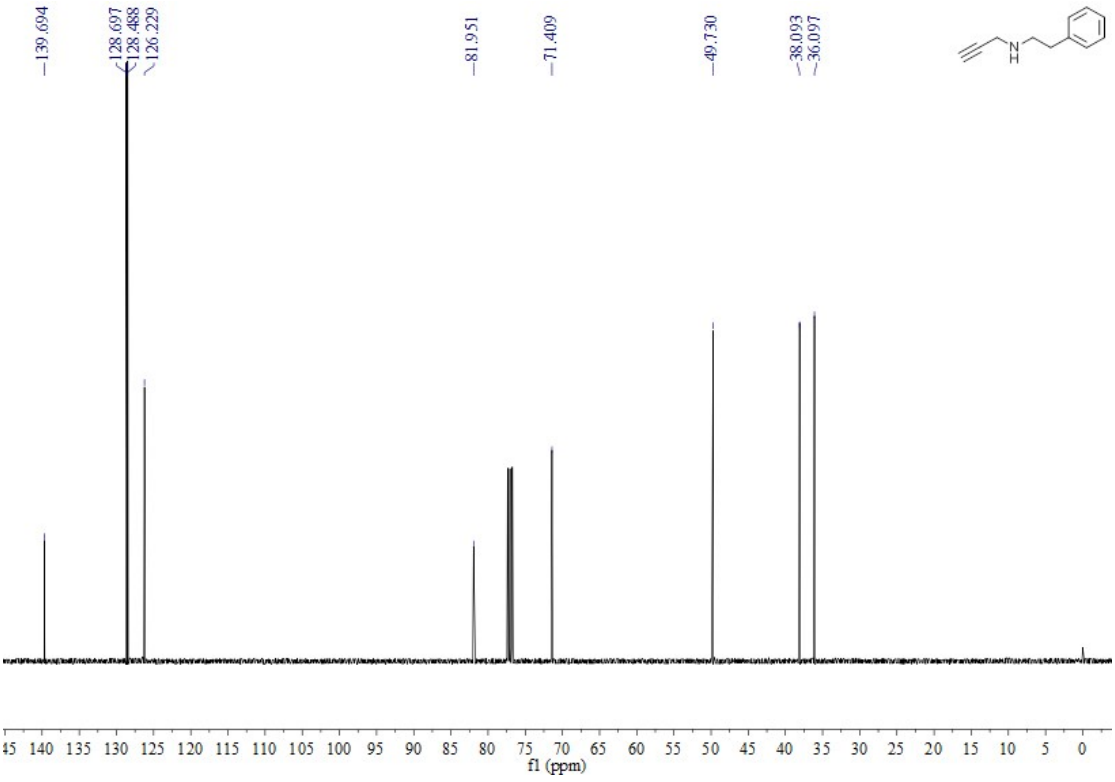
139.694
128.697
128.488
126.229
81.951
71.409
49.730
38.093
36.097
f1 (ppm)

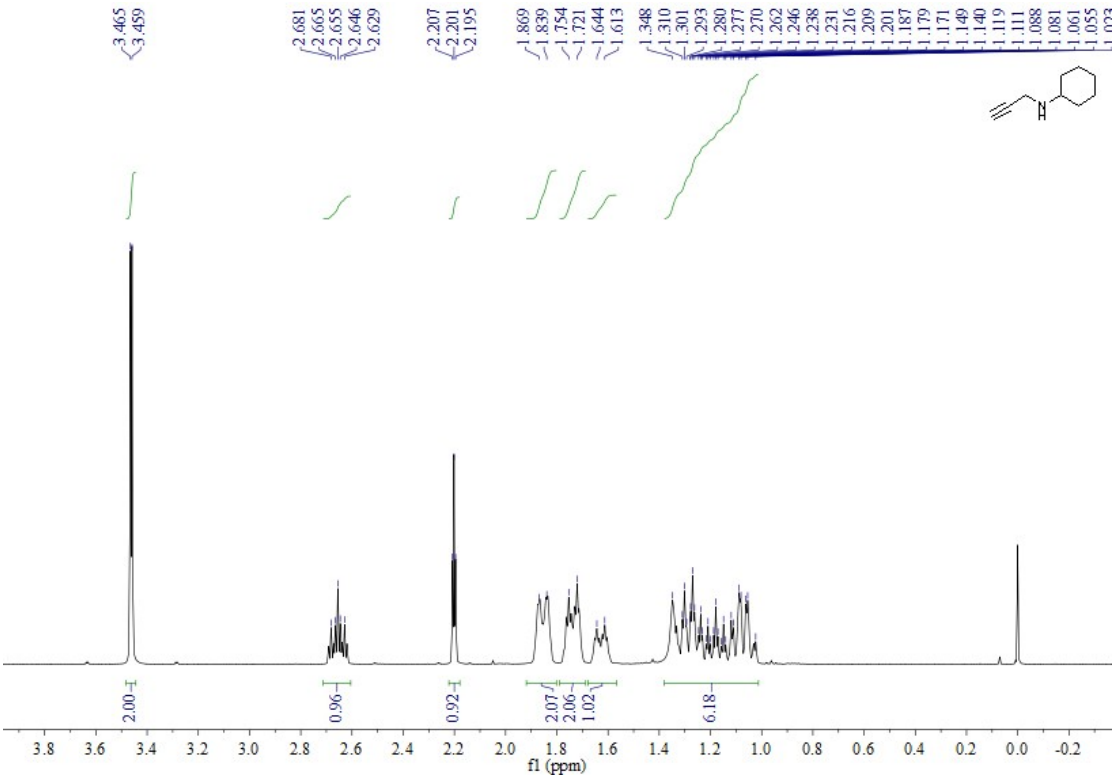
3.465
3.459
2.681
2.665
2.655
2.646
2.629
2.207
2.201
2.195
1.869
1.839
1.754
1.721
1.644
1.613
1.348
1.310
1.301
1.293
1.280
1.277
1.270
1.262
1.246
1.238
1.231
1.216
1.209
1.201
1.187
1.179
1.171
1.149
1.140
1.119
1.111
1.088
1.081
1.061
1.055
2.00
0.96
0.92
2.07
2.06
1.02
6.18
f1 (ppm)

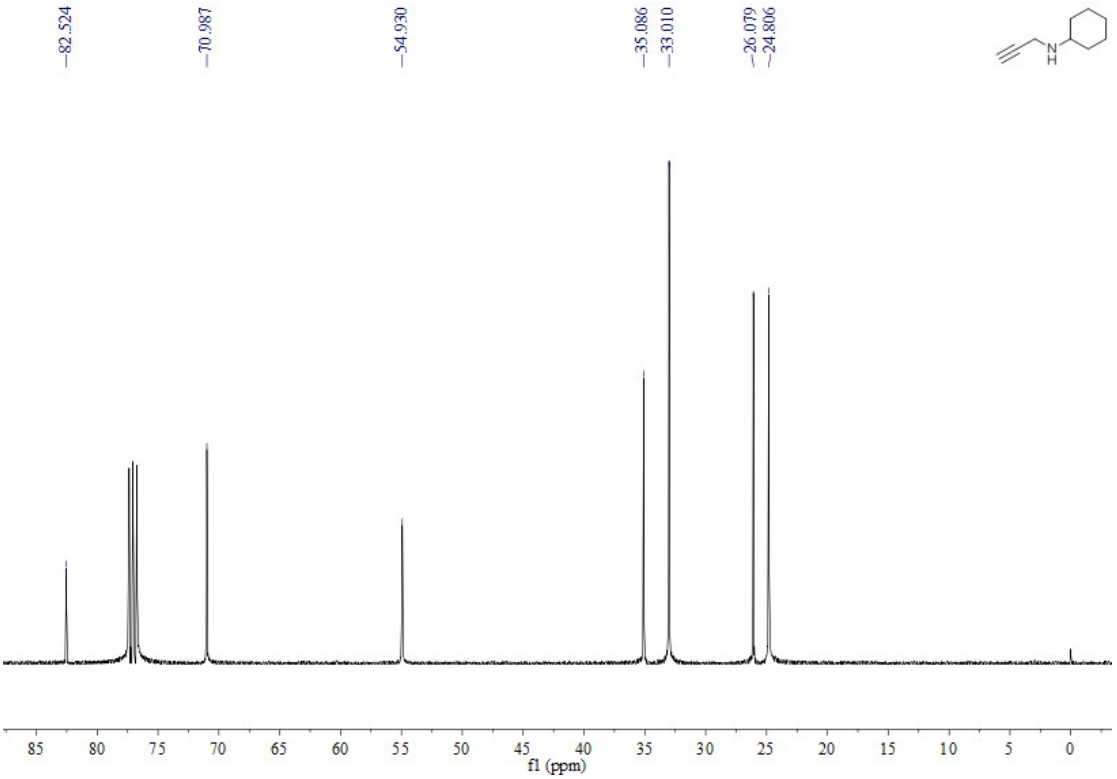
82.524
70.987
54.930
35.086
33.010
26.079
24.806
f1 (ppm)

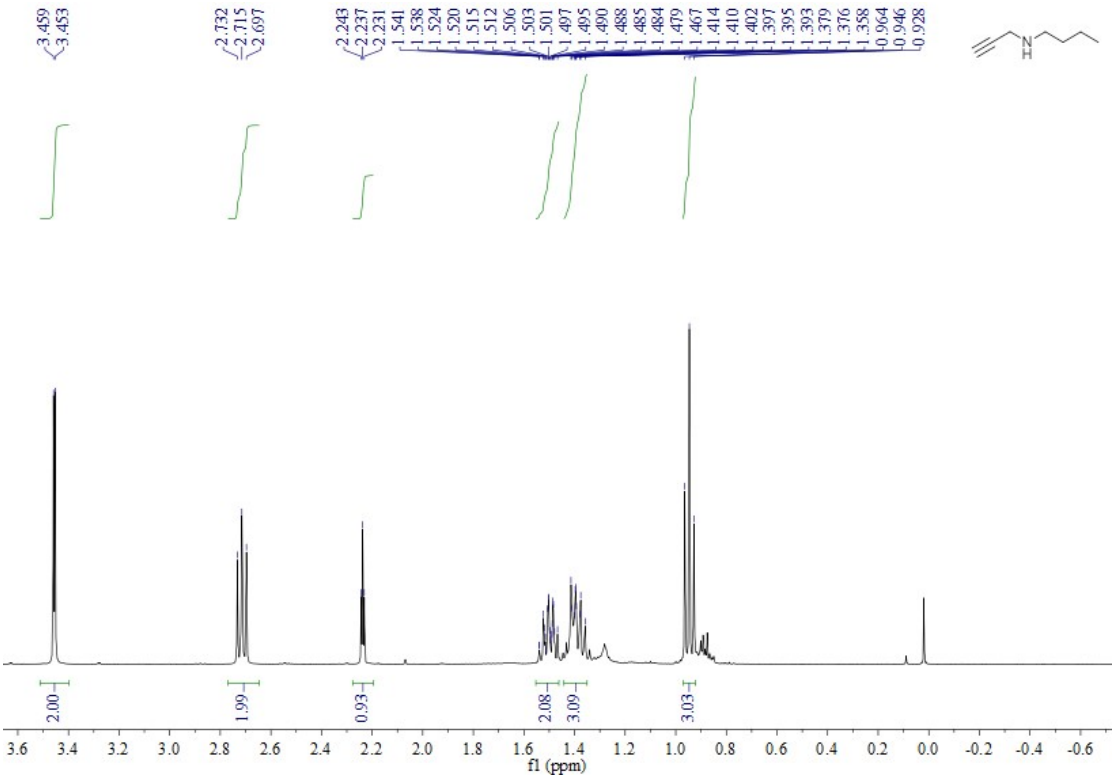
3.459
3.453
2.732
2.715
2.697
2.243
2.237
2.231
1.541
1.538
1.524
1.520
1.515
1.512
1.506
1.503
1.501
1.497
1.495
1.490
1.488
1.485
1.484
1.479
1.467
1.414
1.410
1.402
1.397
1.395
1.393
1.379
1.376
1.358
0.964
0.946
0.928
2.00
1.99
0.93
2.08
3.09
3.03
f1 (ppm)

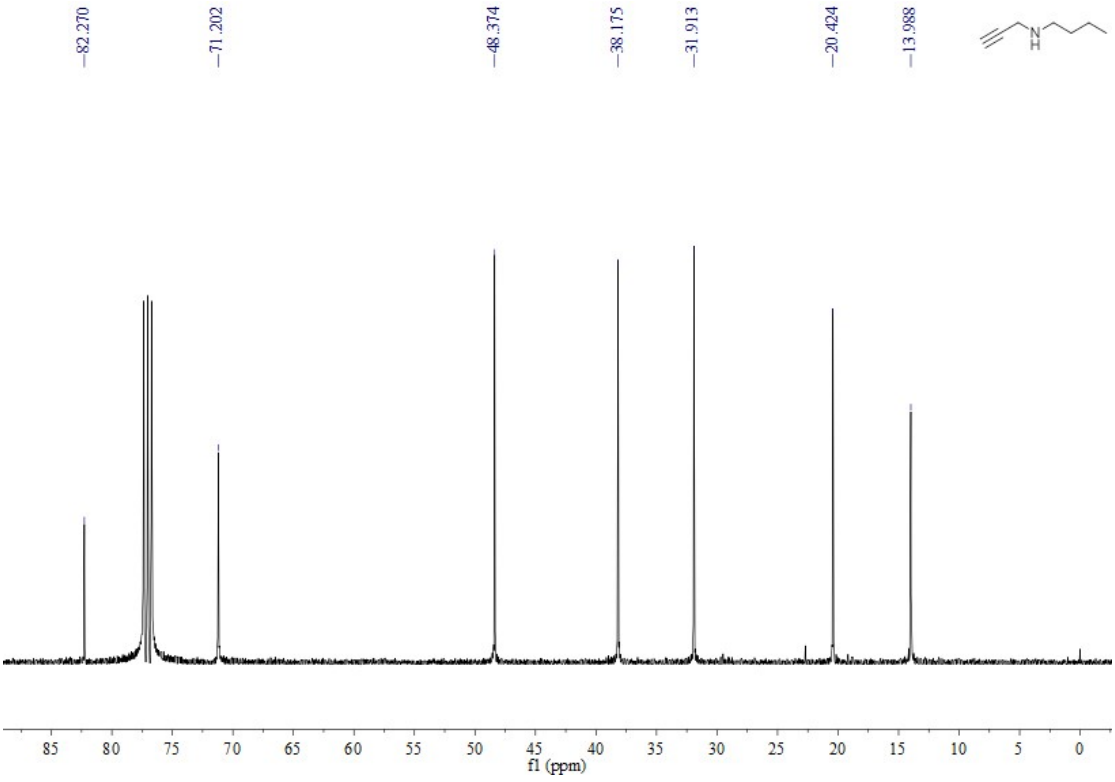
82.270
71.202
48.374
38.175
31.913
20.424
13.988
f1 (ppm)

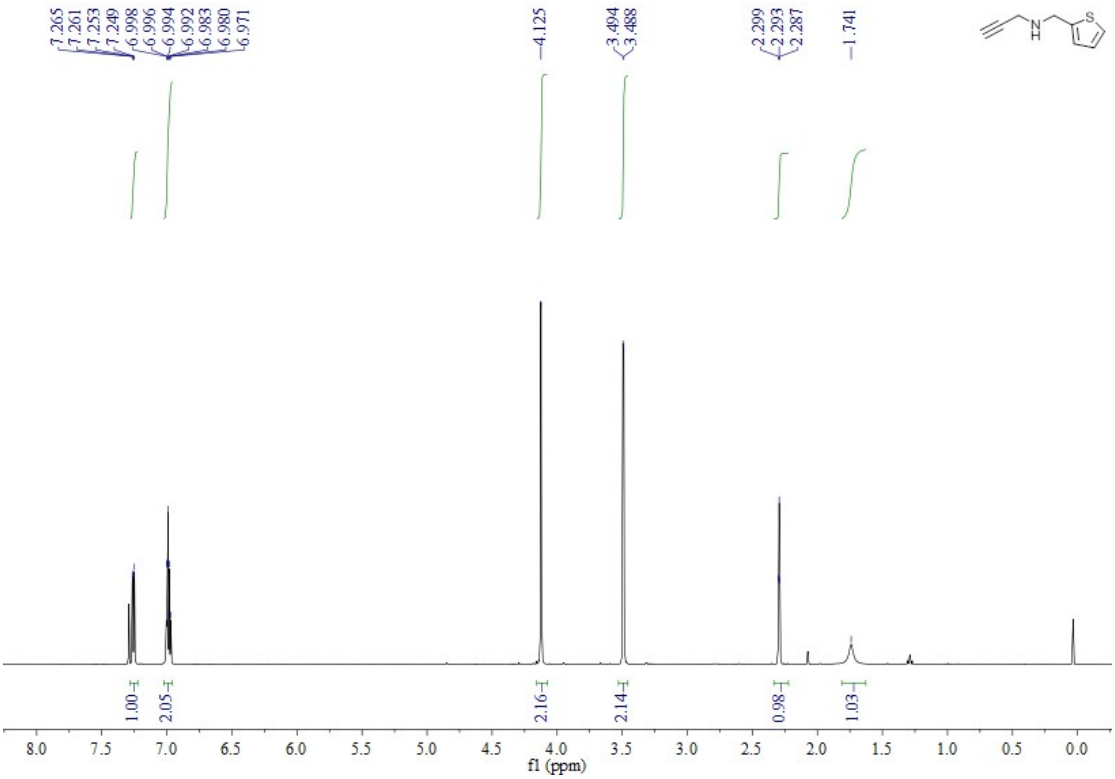
7.265
7.261
7.253
7.249
6.998
6.996
6.994
6.992
6.983
6.980
6.971
4.125
3.494
3.488
2.299
2.293
2.287
1.741
1.00
2.05
2.16
2.14
0.98
1.03
f1 (ppm)

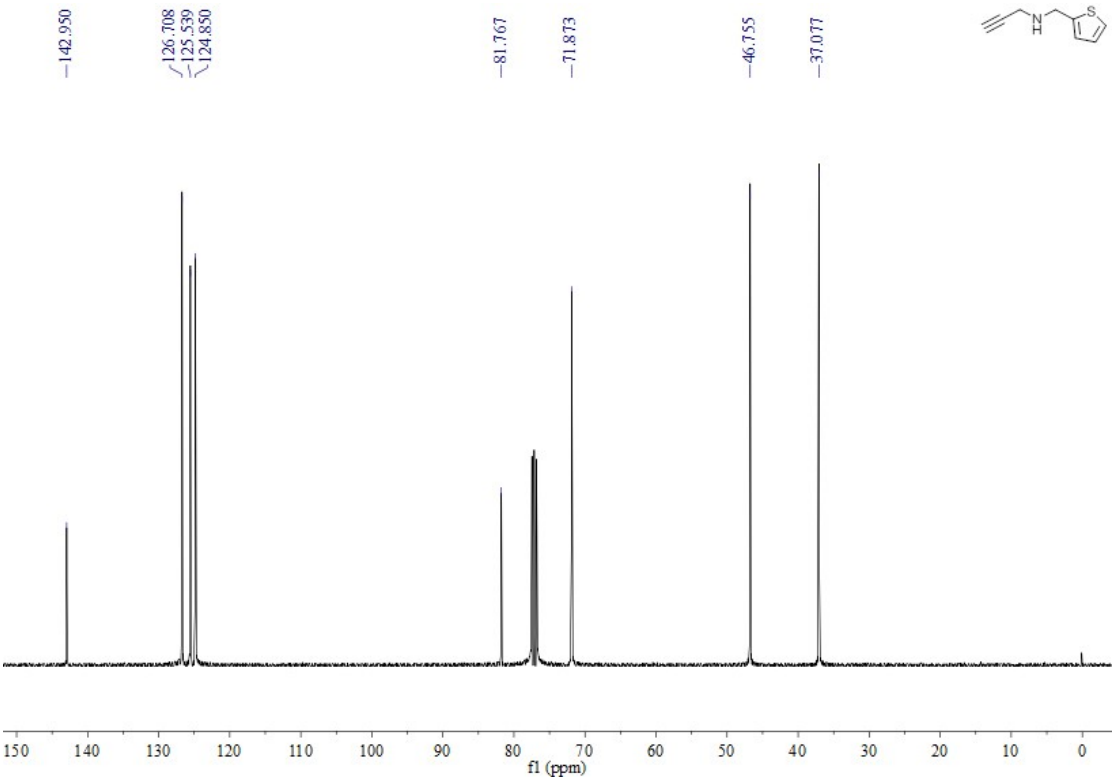
142.950
126.708
125.539
124.850
81.767
71.873
46.755
37.077
f1 (ppm)

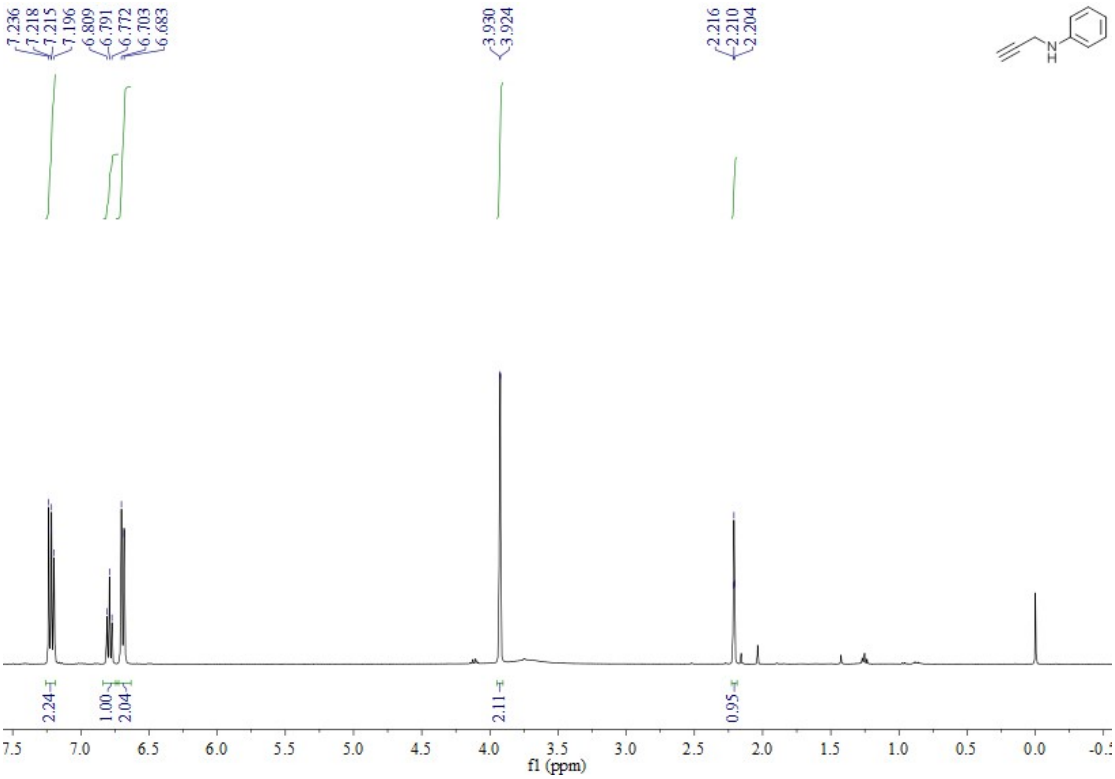
7.236
7.218
7.215
7.196
6.809
6.791
6.772
6.703
6.683
3.930
3.924
2.216
2.210
2.204
2.24
1.00
2.04
2.11
0.95
f1 (ppm)

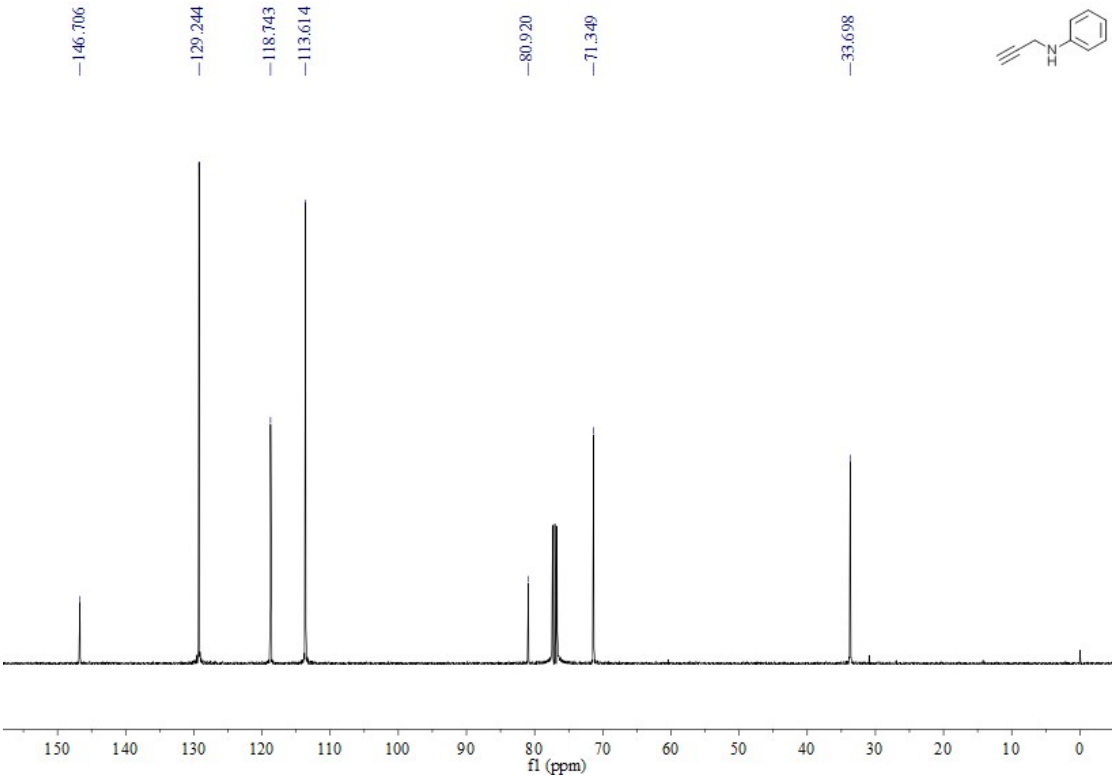
146.706
129.244
118.743
113.614
80.920
71.349
33.698
f1 (ppm)

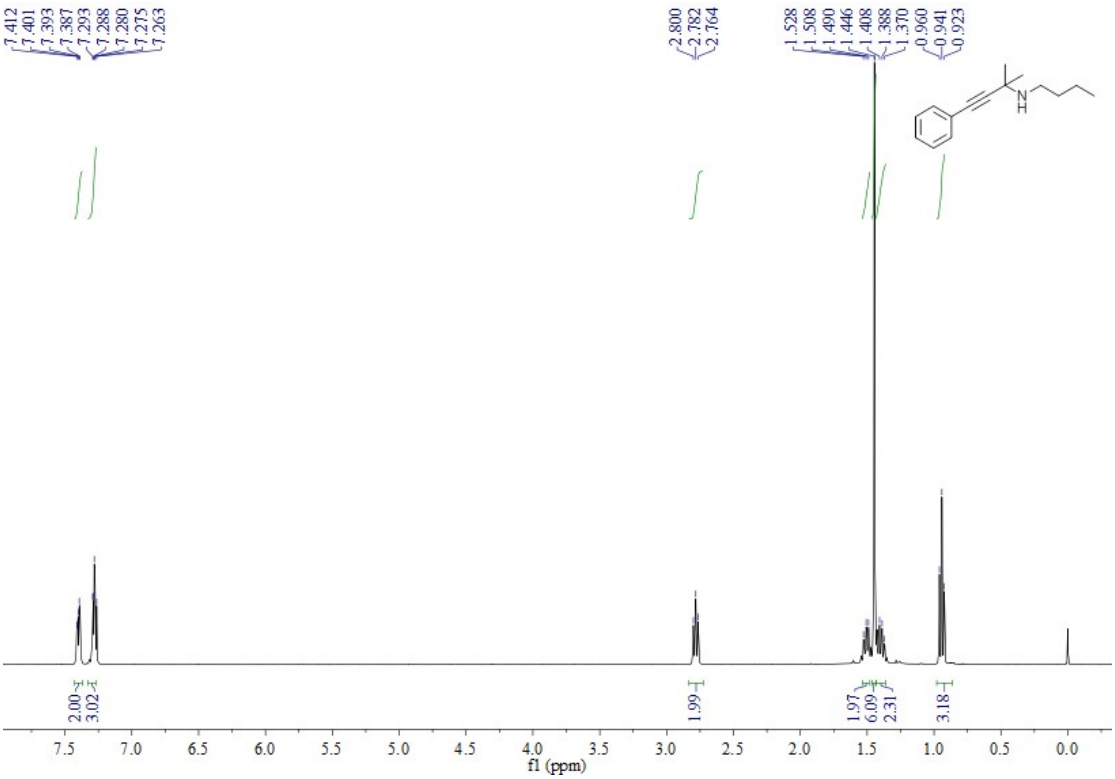
7.412
7.401
7.393
7.387
7.293
7.288
7.280
7.275
7.263
2.800
2.782
2.764
1.528
1.508
1.490
1.446
1.408
1.388
1.370
0.960
0.941
0.923
2.00
3.02
1.99
1.97
6.09
2.31
3.18
f1 (ppm)

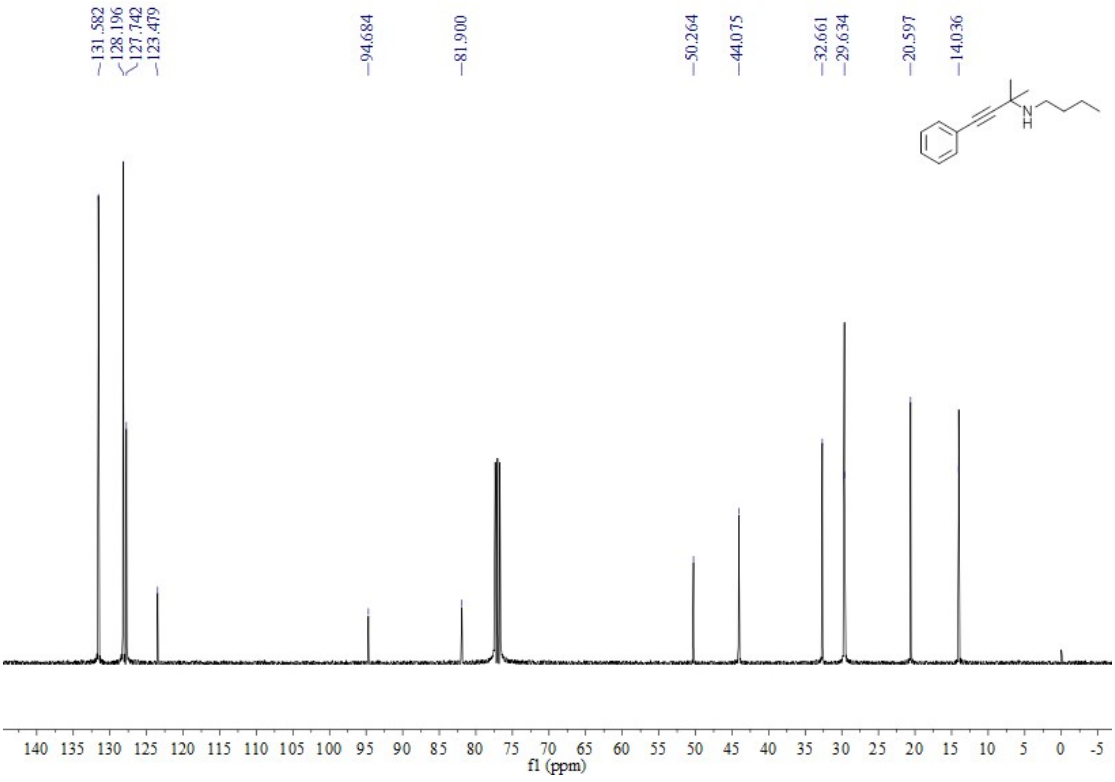
131.582
128.196
127.742
123.479
94.684
81.900
50.264
44.075
32.661
29.634
20.597
14.036
f1 (ppm)

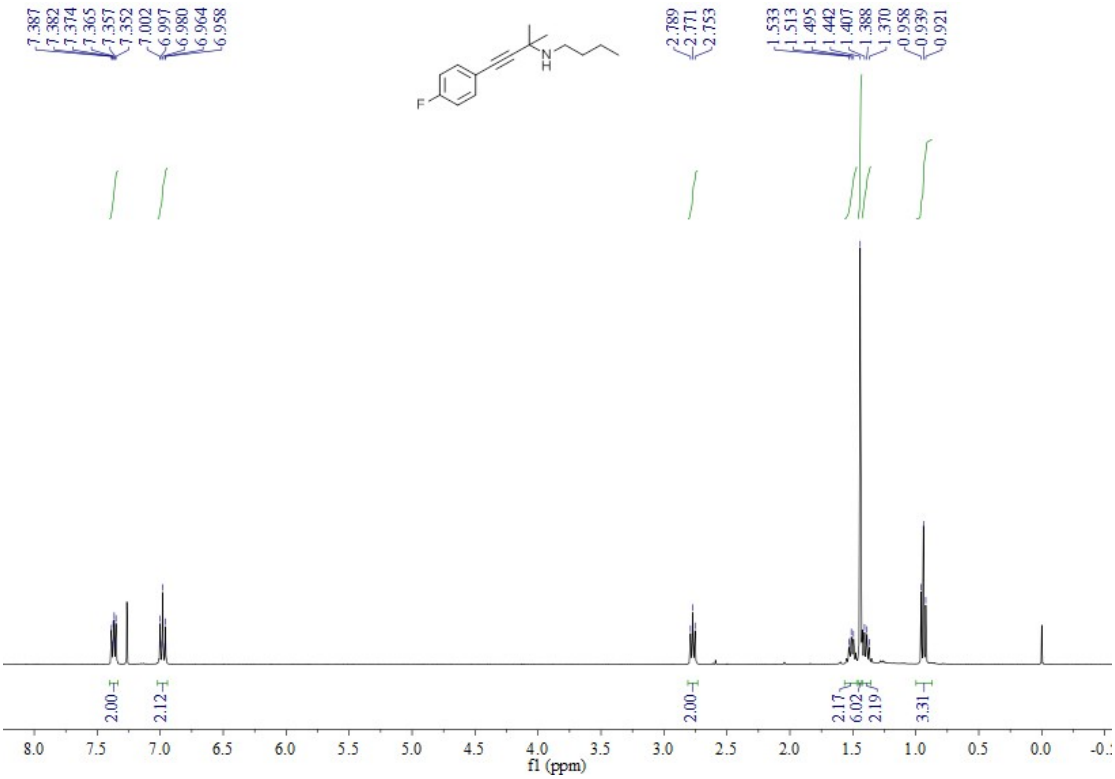
7.387
7.382
7.374
7.365
7.357
7.352
7.002
6.997
6.980
6.964
6.958
2.789
2.771
2.753
1.533
1.513
1.495
1.442
1.407
1.388
1.370
0.958
0.939
0.921
F
NH
2.00
2.12
2.00
2.17
6.02
2.19
3.31
f1 (ppm)

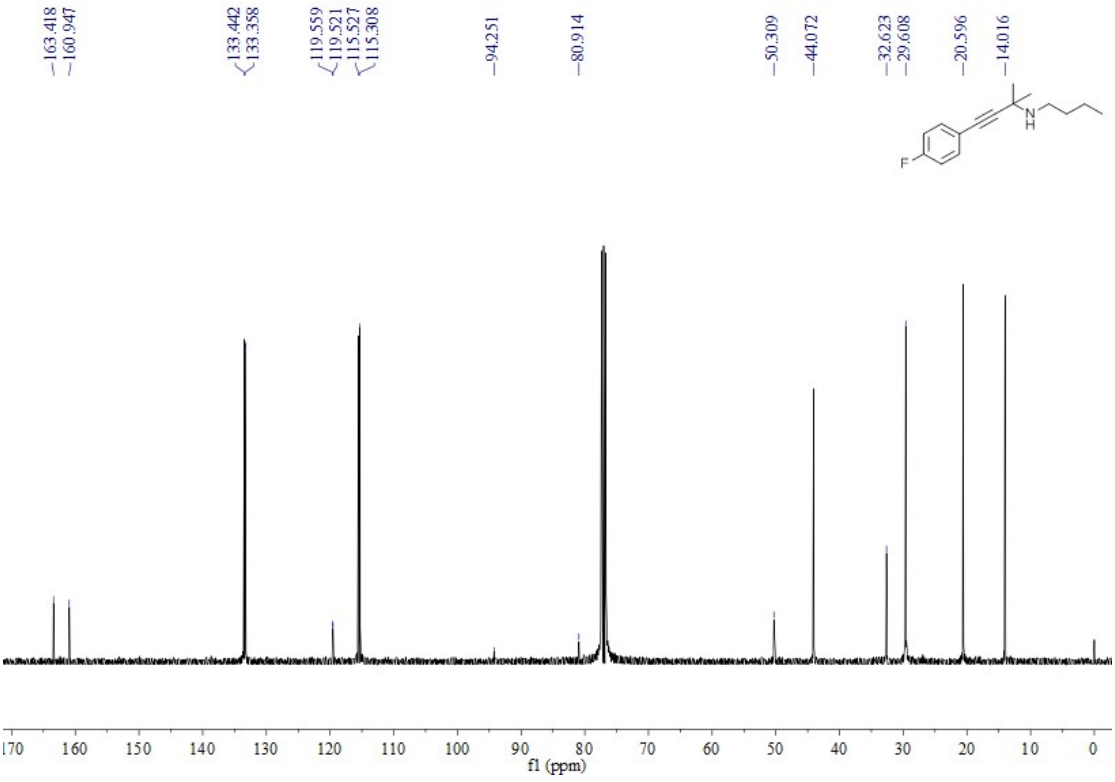
163.418
160.947
133.442
133.358
119.559
119.521
115.527
115.308
94.251
80.914
50.309
44.072
32.623
29.608
20.596
14.016
F
NH
f1 (ppm)

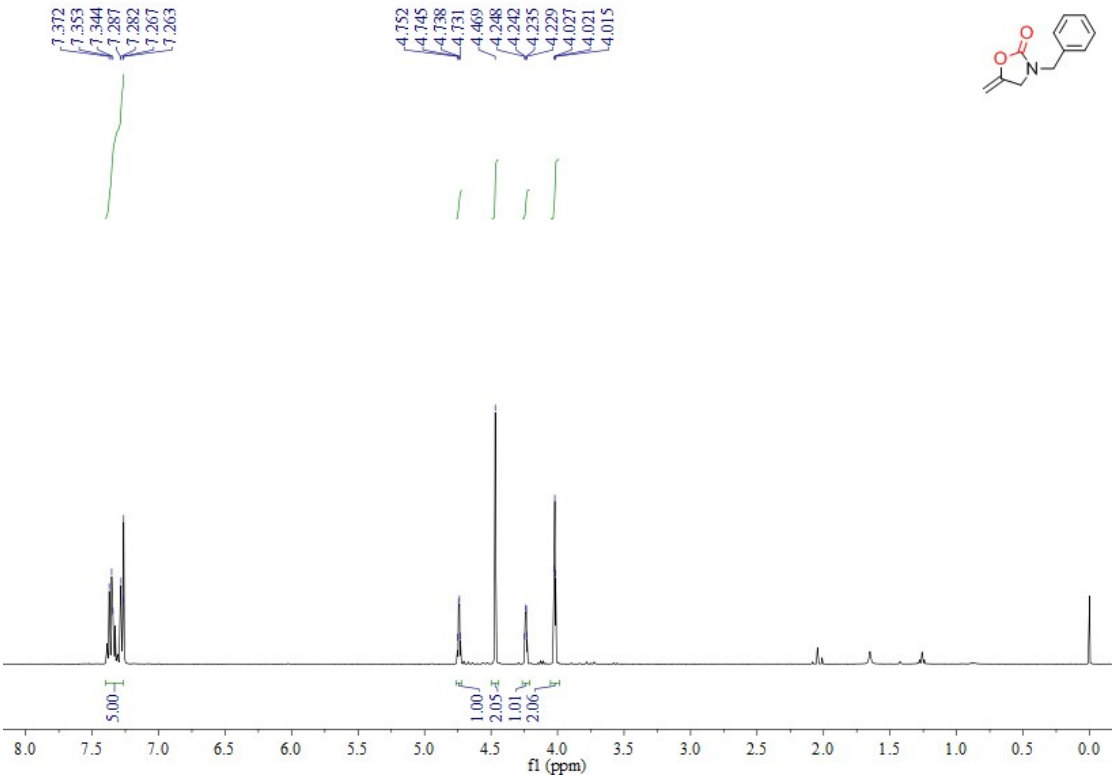
7.372
7.353
7.344
7.287
7.282
7.267
7.263
4.752
4.745
4.738
4.731
4.469
4.248
4.242
4.235
4.229
4.027
4.021
4.015
5.00
1.00
2.05
1.01
2.06
f1 (ppm)

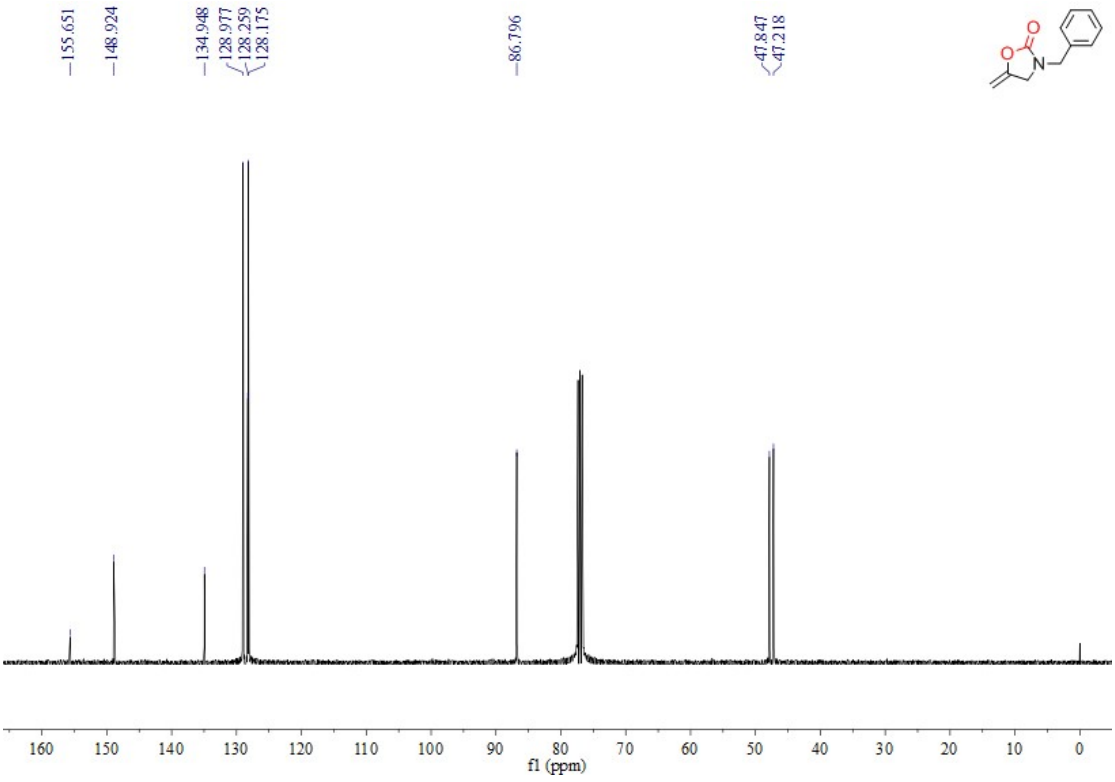
155.651
148.924
134.948
128.977
128.259
128.175
86.796
47.847
47.218
f1 (ppm)

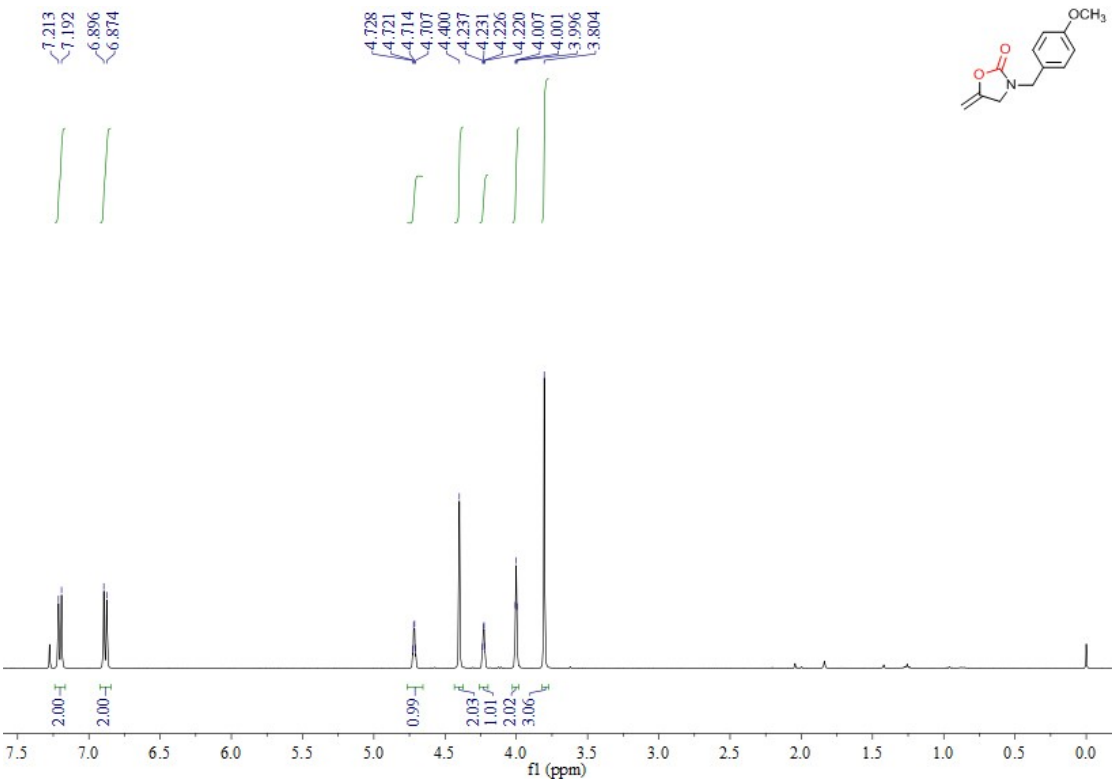
7.213
7.192
6.896
6.874
4.728
4.721
4.714
4.707
4.400
4.237
4.231
4.226
4.220
4.007
4.001
3.996
3.804
OCH3
2.00
2.00
0.99
2.03
1.01
2.02
3.06
f1 (ppm)

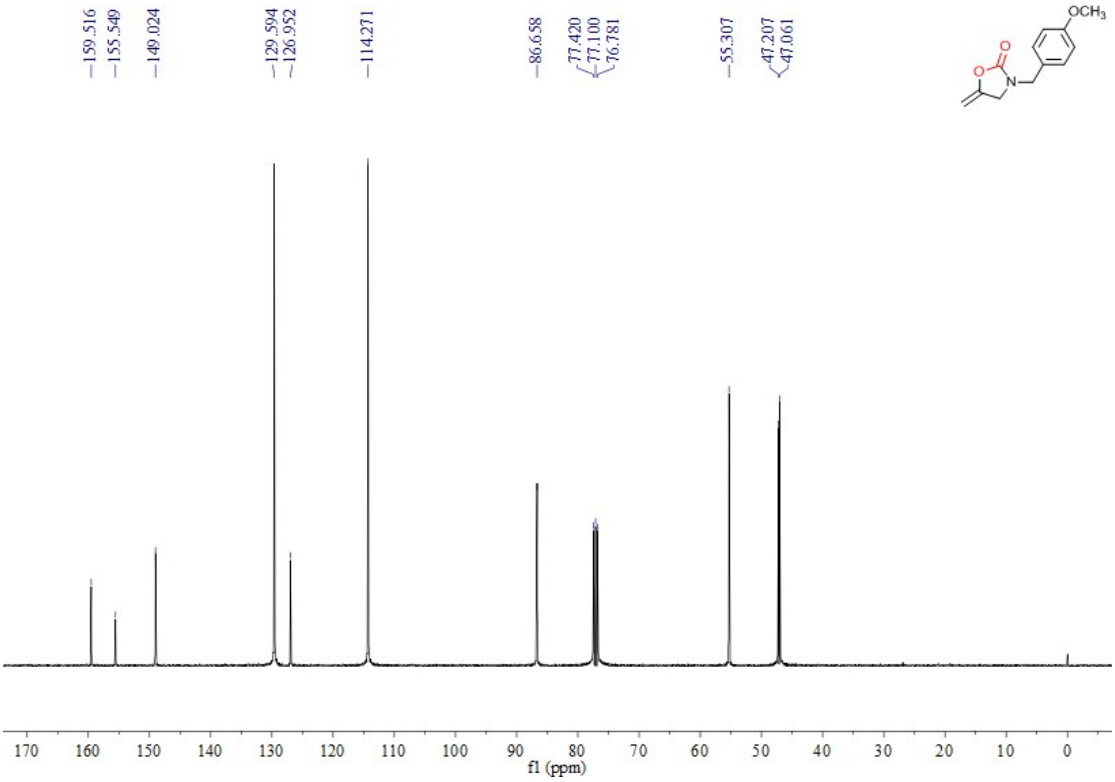
159.516
155.549
149.024
129.594
126.952
114.271
86.658
77.420
77.100
76.781
55.307
47.207
47.061
OCH3
f1 (ppm)

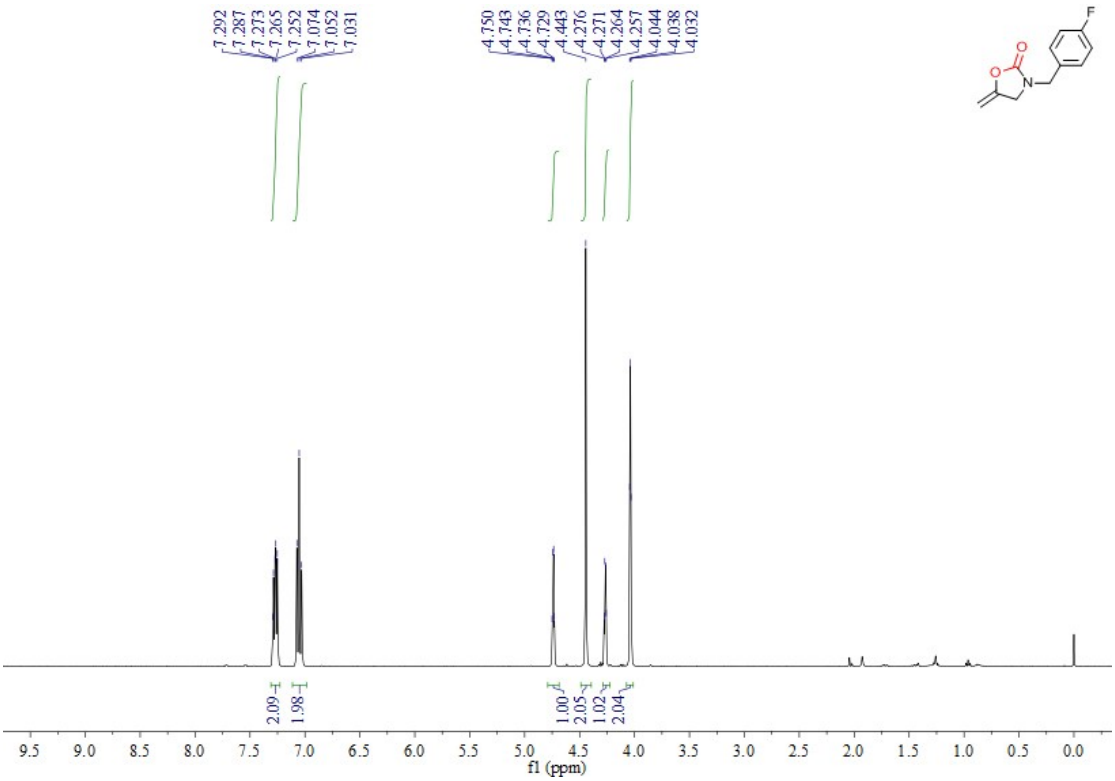
7.292
7.287
7.273
7.265
7.252
7.074
7.052
7.031
4.750
4.743
4.736
4.729
4.443
4.276
4.271
4.264
4.257
4.044
4.038
4.032
F
O
O
N
2.09
1.98
1.00
2.05
1.02
2.04
f1 (ppm)

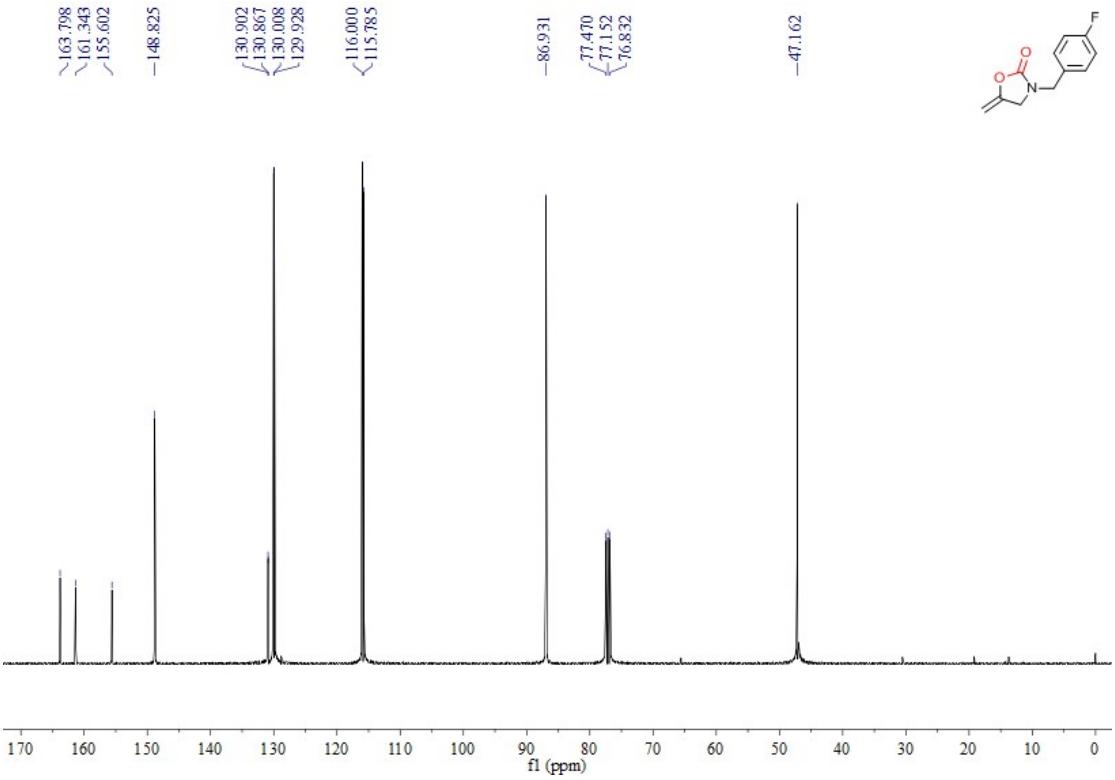
163.798
161.343
155.602
148.825
130.902
130.867
130.008
129.928
116.000
115.785
86.931
77.470
77.152
76.832
47.162
F
O
O
N
f1 (ppm)

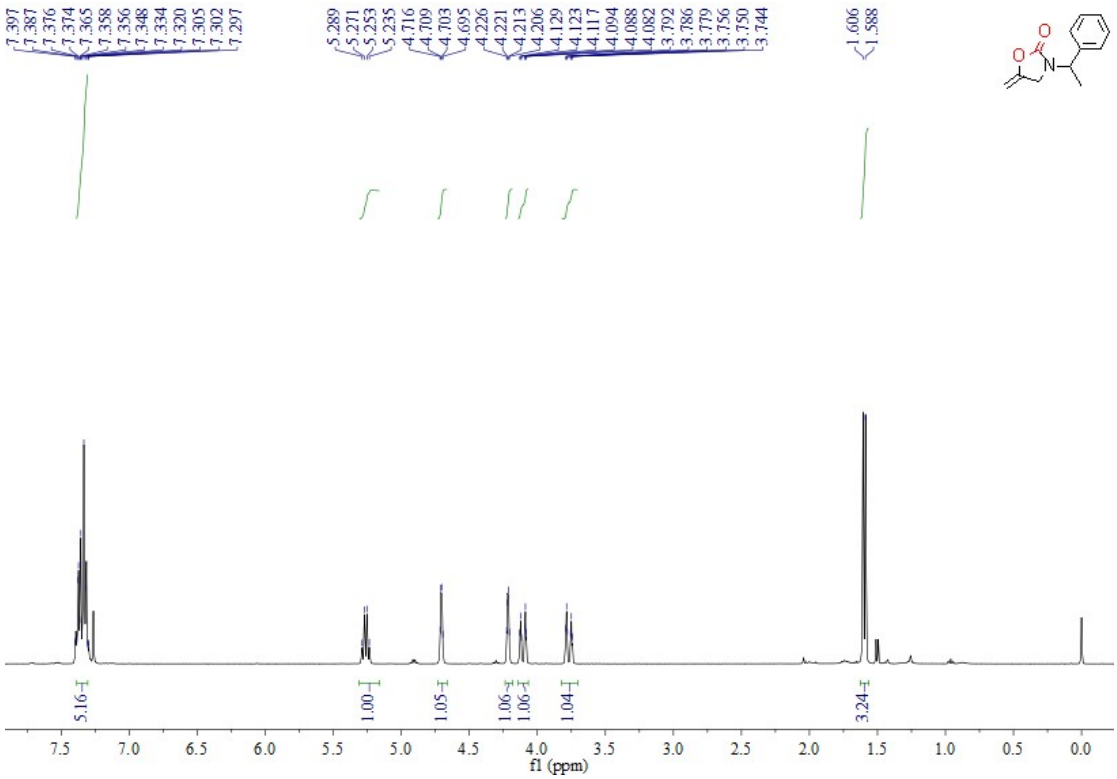
7.397
7.387
7.376
7.374
7.365
7.358
7.356
7.348
7.334
7.320
7.305
7.302
7.297
5.289
5.271
5.253
5.235
4.716
4.709
4.703
4.695
4.226
4.221
4.213
4.206
4.129
4.123
4.117
4.094
4.088
4.082
3.792
3.786
3.779
3.756
3.750
3.744
1.606
1.588
5.16
1.00
1.05
1.06
1.06
1.04
3.24
f1 (ppm)

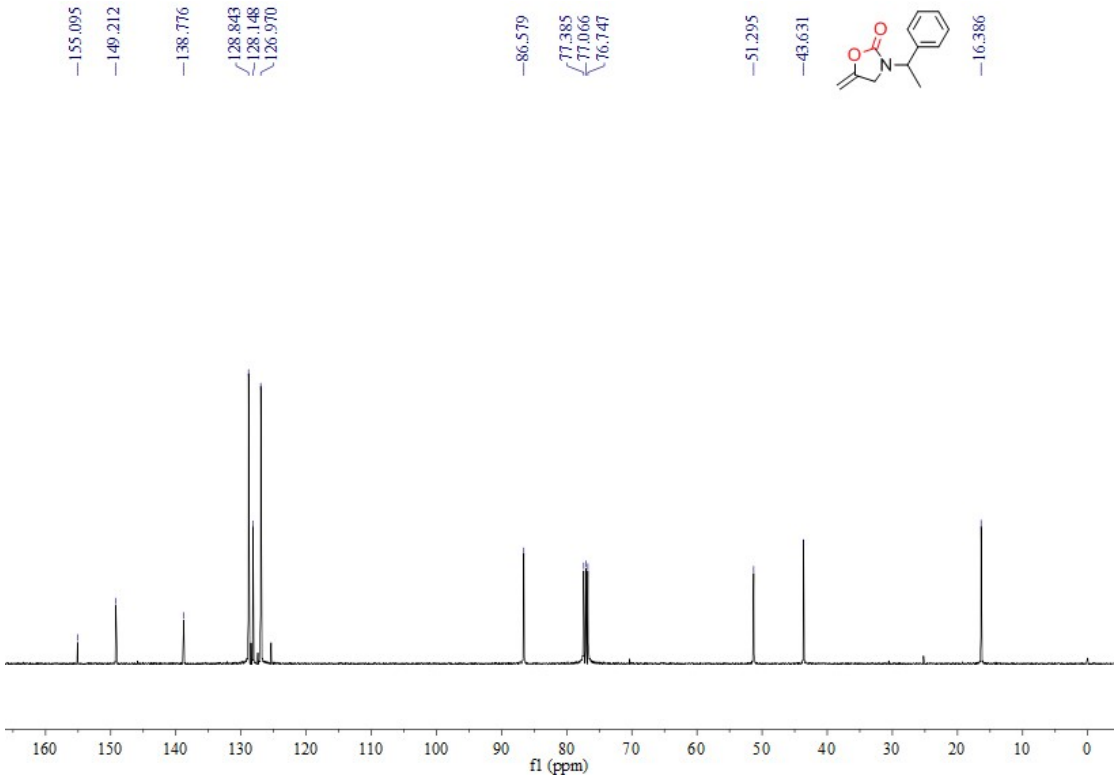
155.095
149.212
138.776
128.843
128.148
126.970
86.579
77.385
77.066
76.747
51.295
43.631
16.386
f1 (ppm)

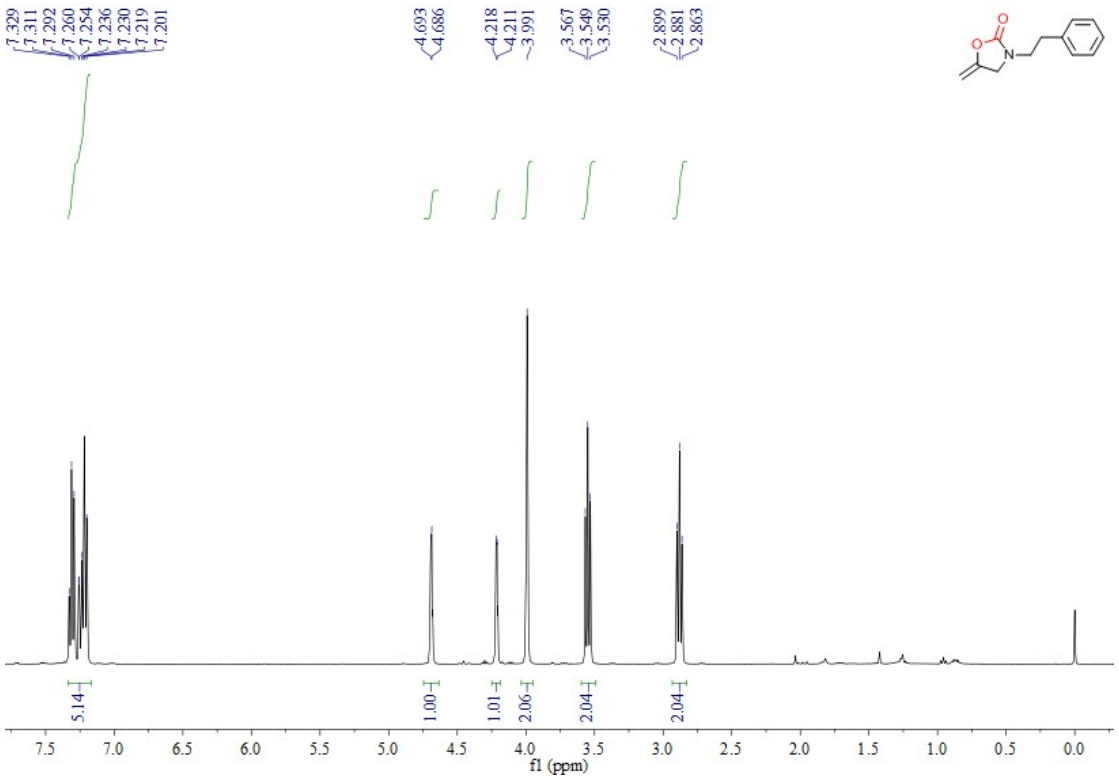
7.329
7.311
7.292
7.260
7.254
7.236
7.230
7.219
7.201
4.693
4.686
4.218
4.211
3.991
3.567
3.549
3.530
2.899
2.881
2.863
5.14
1.00
1.01
2.06
2.04
2.04
f1 (ppm)

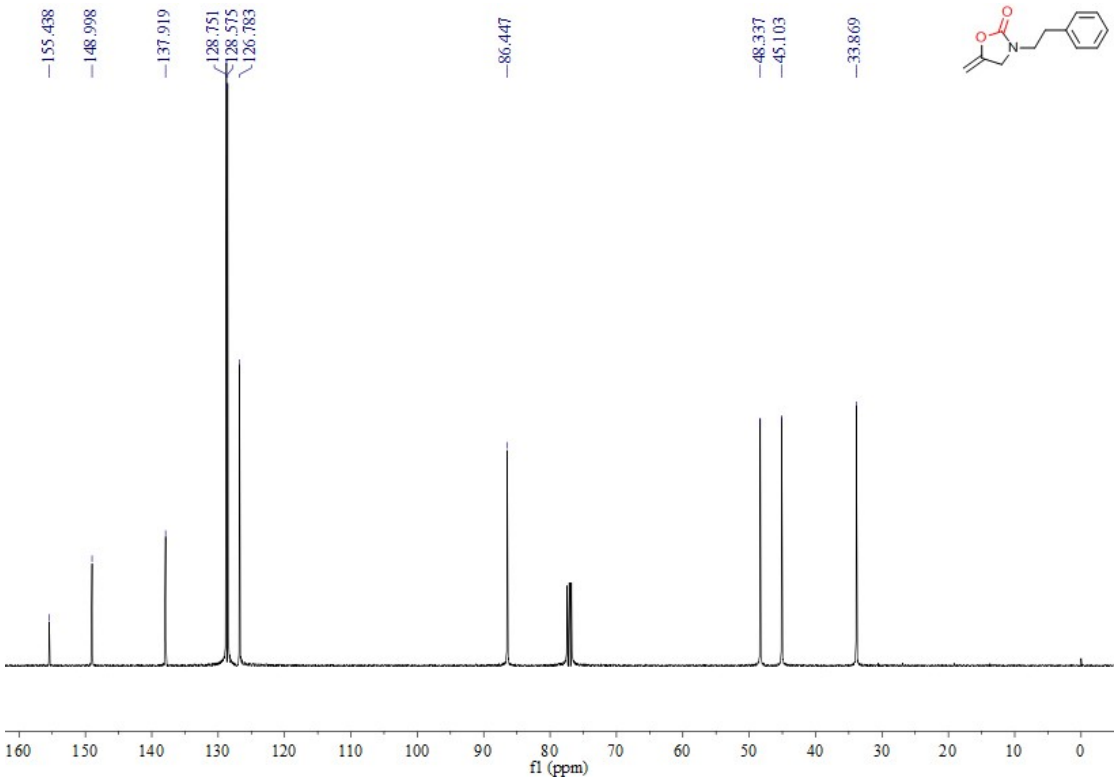
155.438
148.998
137.919
128.751
128.575
126.783
86.447
48.337
45.103
33.869
f1 (ppm)

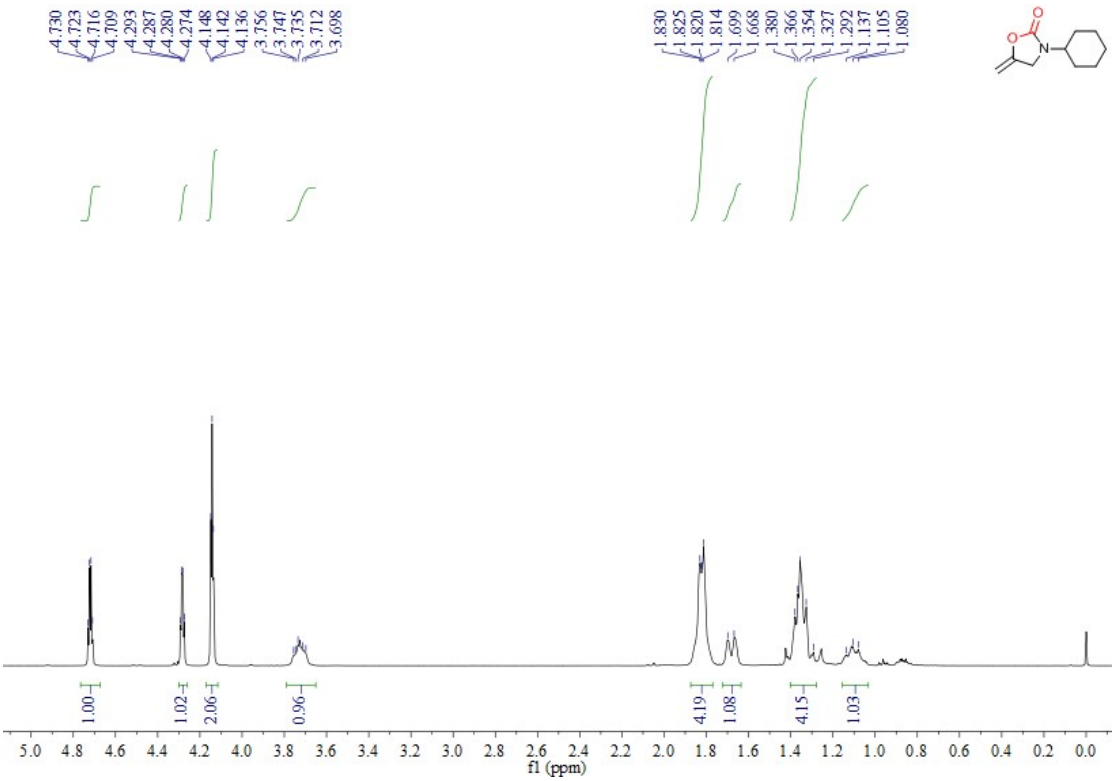
4.730
4.723
4.716
4.709
4.293
4.287
4.280
4.274
4.148
4.142
4.136
3.756
3.747
3.735
3.712
3.698
1.830
1.825
1.820
1.814
1.699
1.668
1.380
1.366
1.354
1.327
1.292
1.137
1.105
1.080
1.00
1.02
2.06
0.96
4.19
1.08
4.15
1.03
f1 (ppm)

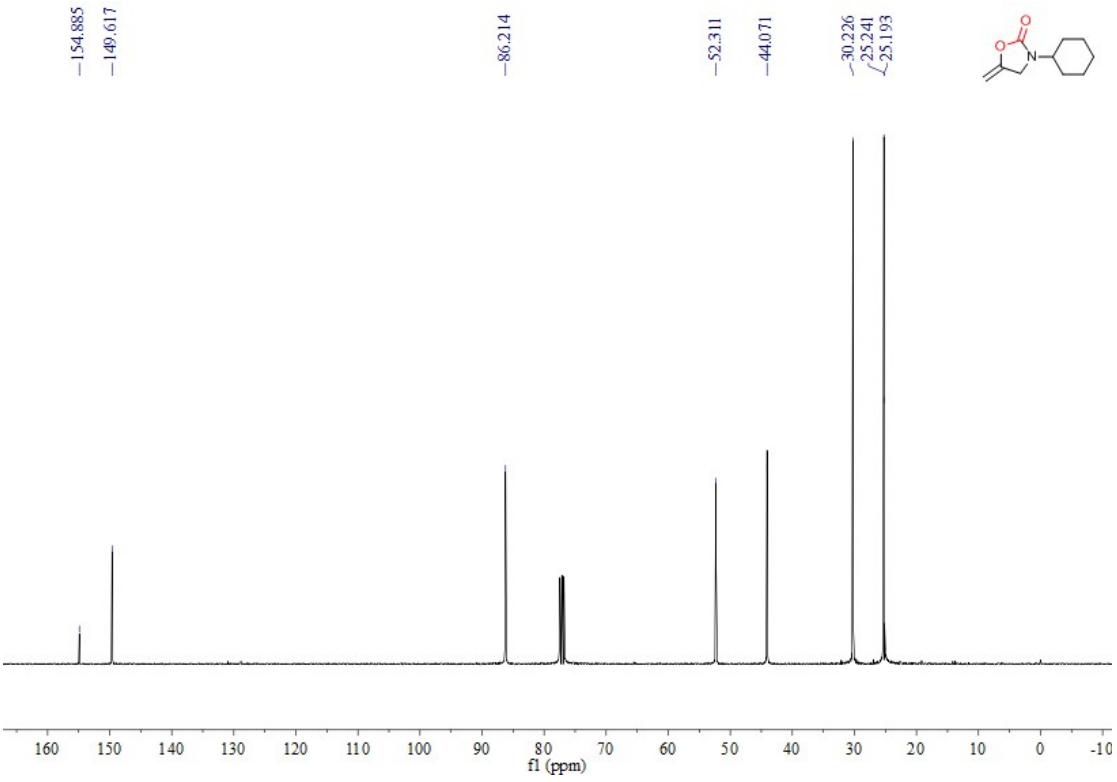
154.885
149.617
86.214
52.311
44.071
30.226
25.241
25.193
f1 (ppm)

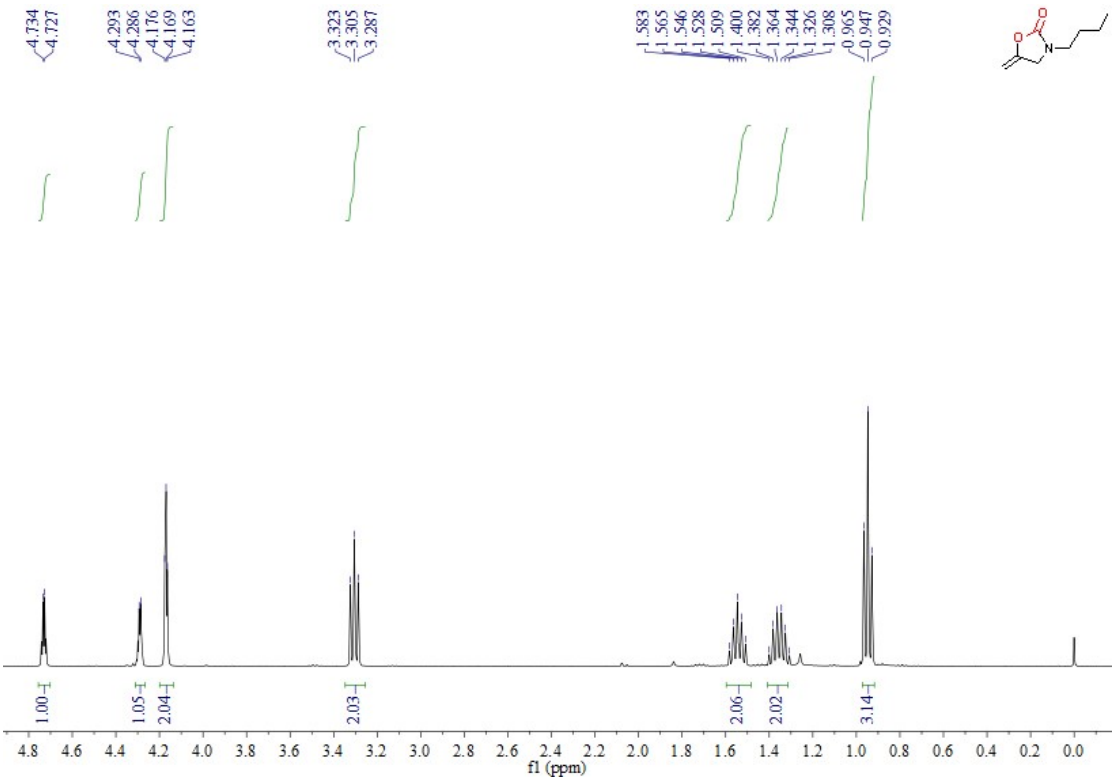
4.734
4.727
4.293
4.286
4.176
4.169
4.163
3.323
3.305
3.287
1.583
1.565
1.546
1.528
1.509
1.400
1.382
1.364
1.344
1.326
1.308
0.965
0.947
0.929
1.00
1.05
2.04
2.03
2.06
2.02
3.14
f1 (ppm)

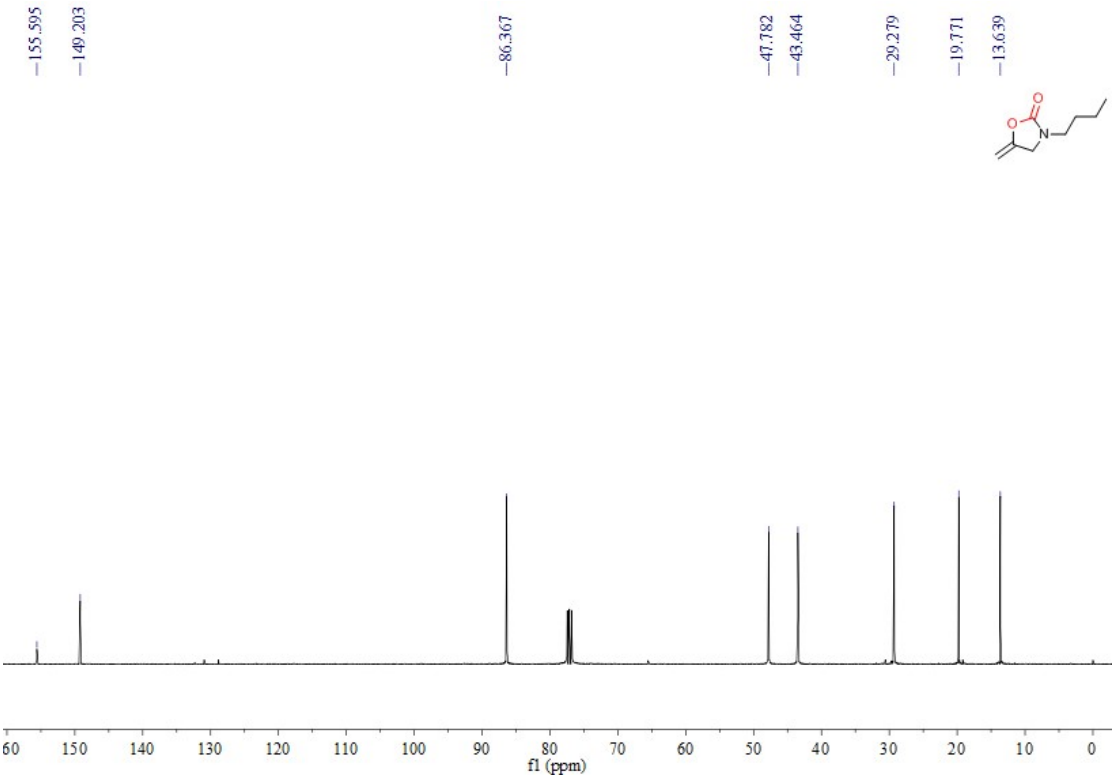
155.595
149.203
86.367
47.782
43.464
29.279
19.771
13.639
f1 (ppm)

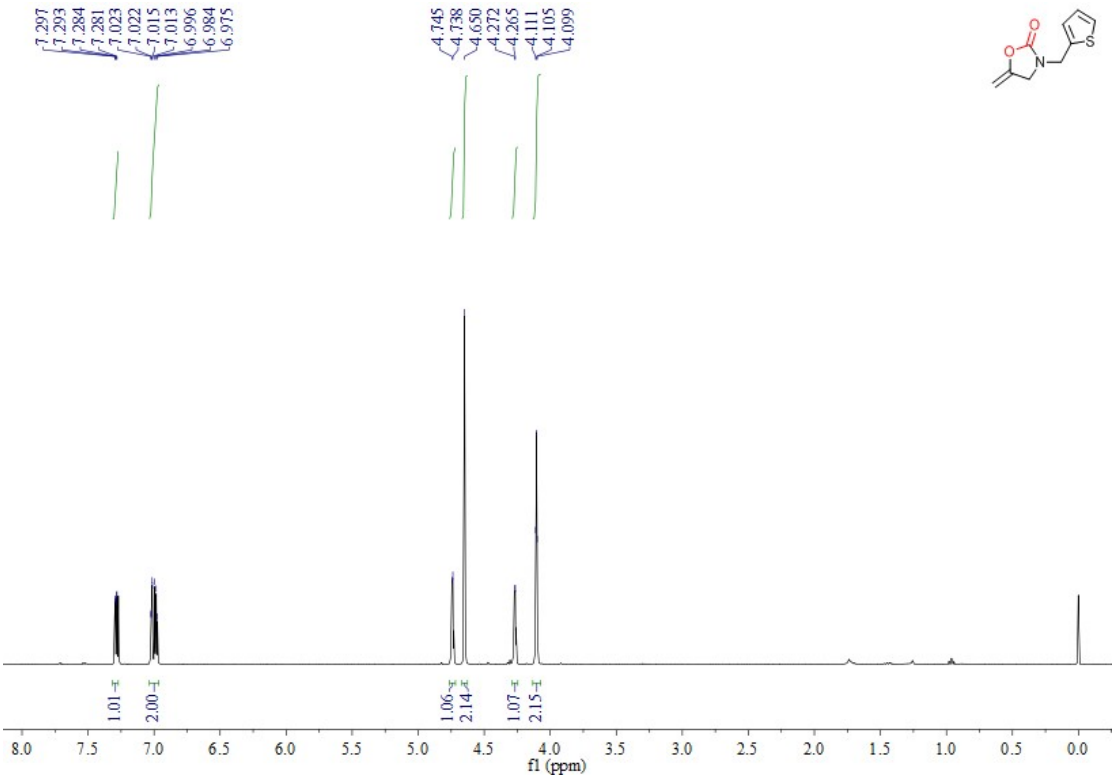
7.297
7.293
7.284
7.281
7.023
7.022
7.015
7.013
6.996
6.984
6.975
4.745
4.738
4.650
4.272
4.265
4.111
4.105
4.099
1.01
2.00
1.06
2.14
1.07
2.15
f1 (ppm)

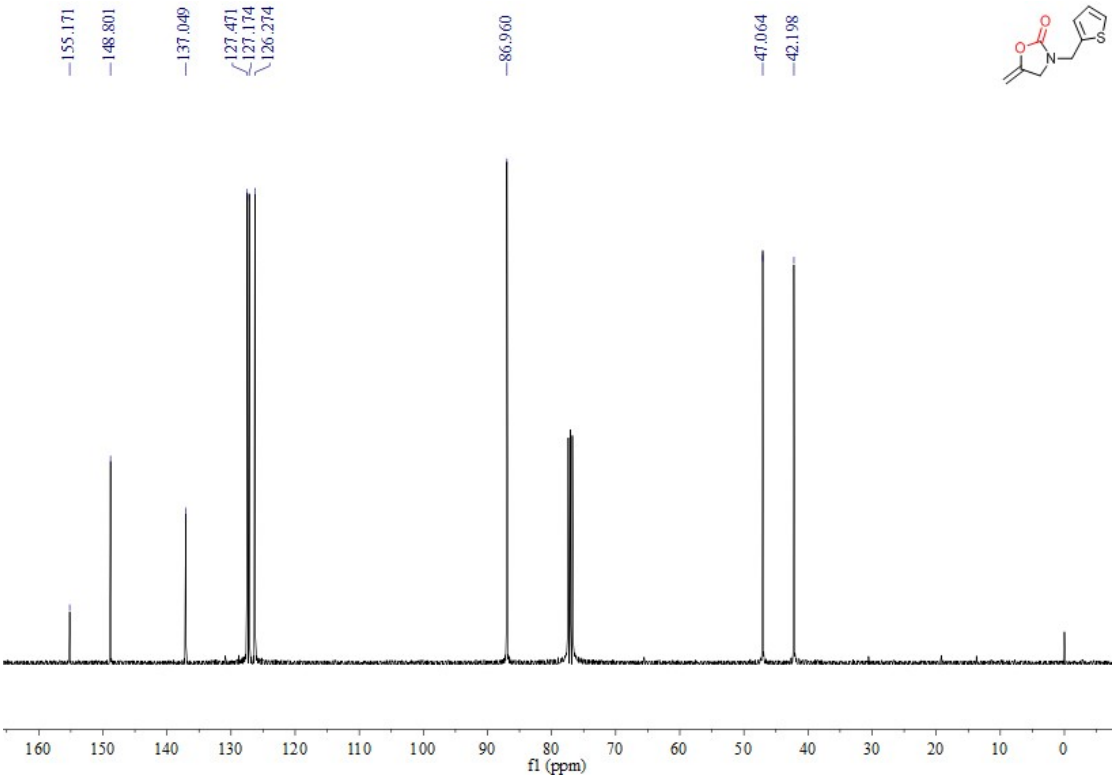
155.171
148.801
137.049
127.471
127.174
126.274
86.960
47.064
42.198
f1 (ppm)

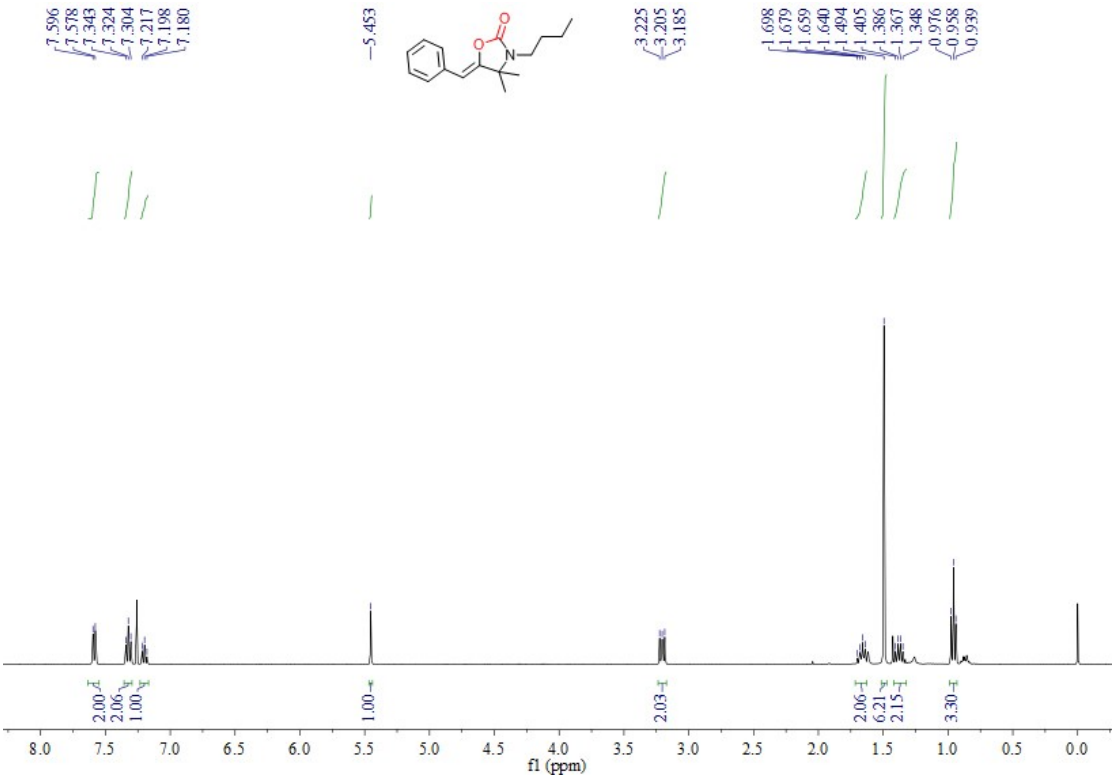
7.596
7.578
7.343
7.324
7.304
7.217
7.198
7.180
5.453
3.225
3.205
3.185
1.698
1.679
1.659
1.640
1.494
1.405
1.386
1.367
1.348
0.976
0.958
0.939
2.00
2.06
1.00
1.00
2.03
2.06
6.21
2.15
3.30
f1 (ppm)

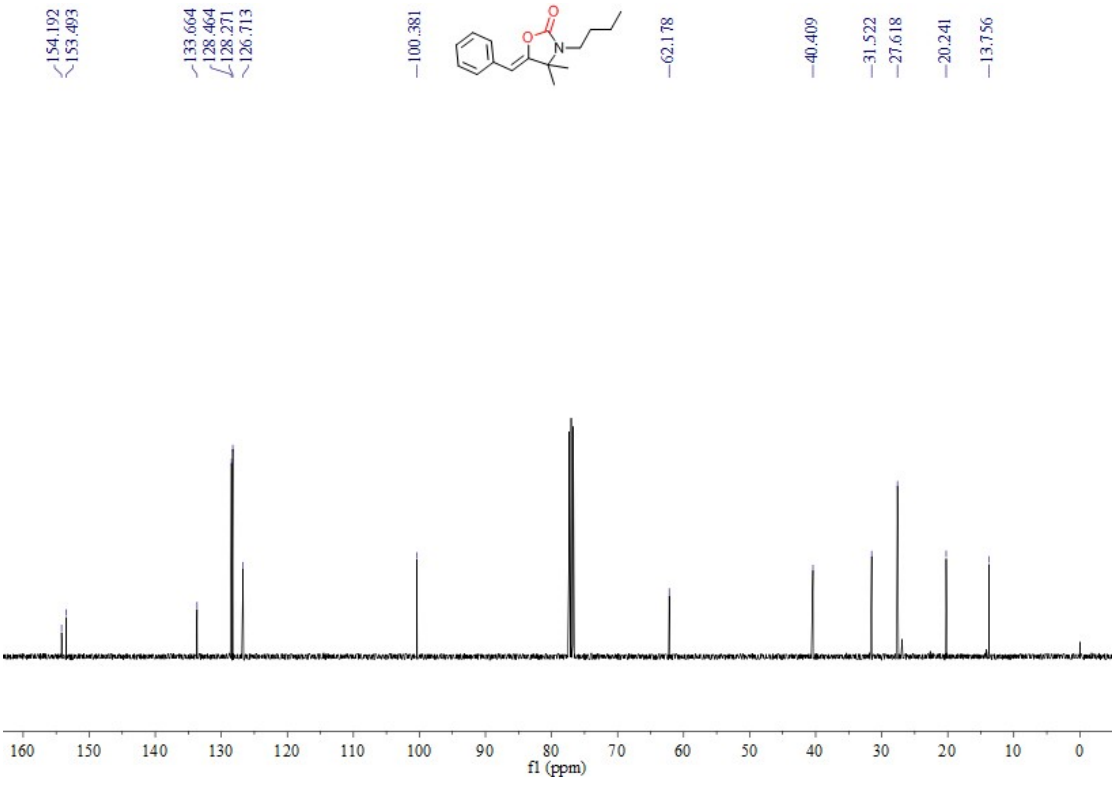
154.192
153.493
133.664
128.464
128.271
126.713
100.381
62.178
40.409
31.522
27.618
20.241
13.756
f1 (ppm)

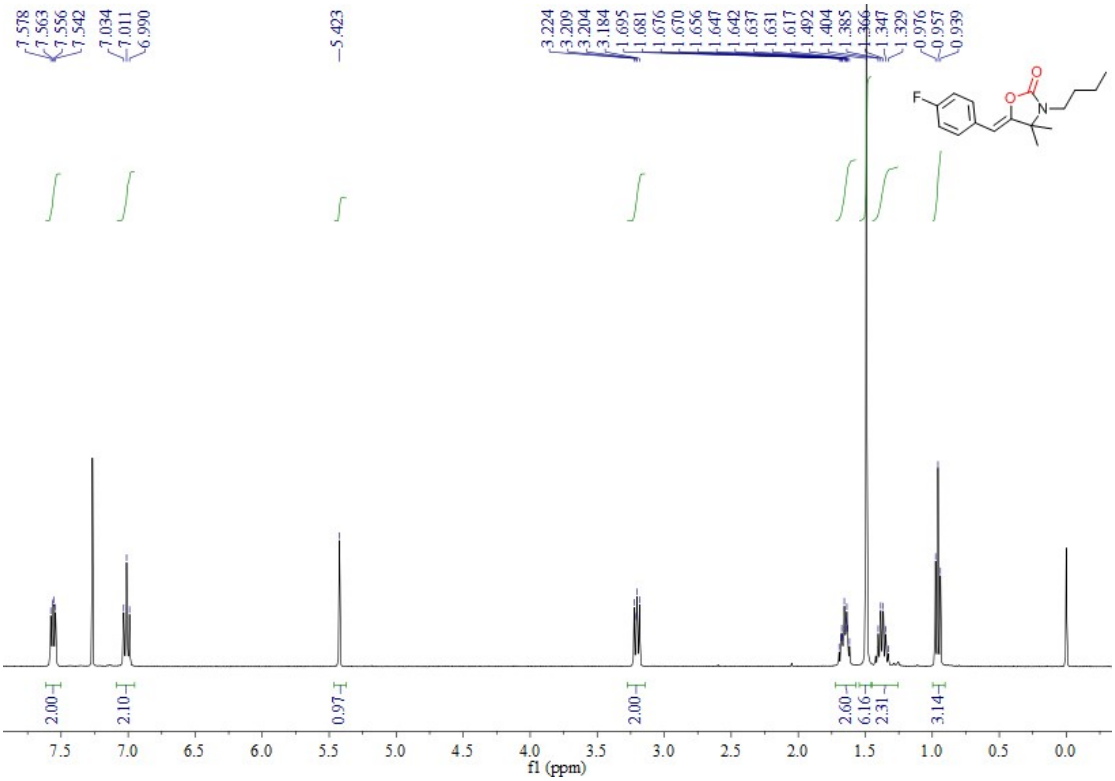
7.578
7.563
7.556
7.542
7.034
7.011
6.990
5.423
3.224
3.209
3.204
3.184
1.695
1.681
1.676
1.670
1.656
1.647
1.642
1.637
1.631
1.617
1.492
1.404
1.385
1.366
1.347
1.329
0.976
0.957
0.939
F
O
O
N
2.00
2.10
0.97
2.00
2.60
6.16
2.31
3.14
7.5
7.0
6.5
6.0
5.5
5.0
4.5
4.0
3.5
3.0
2.5
2.0
1.5
1.0
0.5
0.0
f1 (ppm)

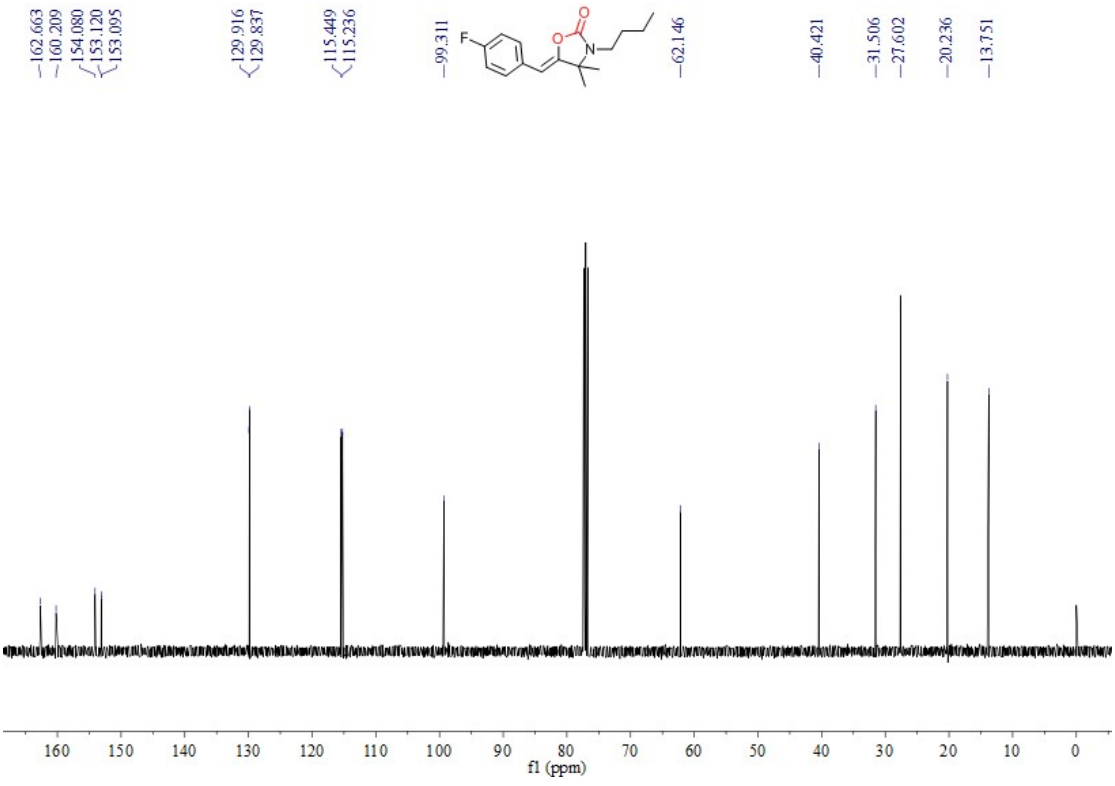
162.663
160.209
154.080
153.120
153.095
129.916
129.837
115.449
115.236
99.311
62.146
40.421
31.506
27.602
20.236
13.751
F
O
O
N
160
150
140
130
120
110
100
90
80
70
60
50
40
30
20
10
0
f1 (ppm)